

AN INVESTIGATION OF LOW ENERGY STRUCTURE
IN NIOBIUM SINGLE CRYSTALS BY SUPERCONDUCTIVE TUNNELING

by

JOHN WILLIAM HAFSTROM

S.B. Massachusetts Institute of Technology
(1965)

Submitted in partial fulfillment of the requirements
for the degree of

DOCTOR OF PHILOSOPHY

at the

Massachusetts Institute of Technology
(1969)

Signature of Author
Department of Metallurgy
and Materials Science

Signature of Professor
in Charge of Research

Signature of Chairman of
Departmental Committee on
Graduate Students

[Handwritten signatures and scribbles on three horizontal lines]

Archives



AN INVESTIGATION OF LOW ENERGY STRUCTURE
IN NIOBIUM SINGLE CRYSTALS BY SUPERCONDUCTIVE TUNNELING

by

JOHN WILLIAM HAFSTROM

Submitted to the Department of Metallurgy and Materials Science
August, 1969, in partial fulfillment of the requirements for the
degree of Doctor of Philosophy.

ABSTRACT

An investigation of low energy superconductive tunneling into very pure single crystal niobium was performed. Lead and indium films, evaporated onto oxide barriers, were used as the probe.

We find evidence for a second energy gap in niobium at $\Delta/10$. The gap is temperature independent and agrees with various theoretical predictions.

Additional new low voltage structure is found in junctions formed with lead, indicative of tunneling processes occurring within the barrier. Various processes are proposed to explain the structure.

Thesis Supervisor: Robert M. Rose

Title: Associate Professor of Metallurgy

TABLE OF CONTENTS

ABSTRACT	ii
LIST OF FIGURES	iv
ACKNOWLEDGEMENTS ,	vi
INTRODUCTION	1
AN INTRODUCTION TO TUNNELING	2
ELECTRON TUNNELING REVISITED	5
MULTIPLE BAND SUPERCONDUCTIVITY	8
INTRODUCTION TO LOW VOLTAGE TUNNELING STRUCTURE	11
THEORY OF LOW VOLTAGE TUNNELING STRUCTURE	13
EXPERIMENTAL	15
CONSIDERATIONS ON THE INSULATING BARRIER	18
RESULTS	21
FURTHER CONSIDERATIONS ON THE SOURCES OF LOW VOLTAGE TUNNELING STRUCTURE	23
DISCUSSION	27
CONCLUSIONS	32
SUGGESTIONS FOR FURTHER INVESTIGATION	33
REFERENCES	34
FIGURES	37
APPENDIX	
CRYOGENICS	55
ELECTRONICS	58
BIOGRAPHICAL	62

LIST OF FIGURES

FIGURE 1:	Quasiparticle Energy Versus Wavenumber.	37
FIGURE 2:	Single Particle Tunneling.	38
FIGURE 3:	Minimum Energy Diagram for the Process Illustrated in Figure 2.	39
FIGURE 4:	(a) The Occupation of Quasiparticle Levels at Finite Temperature.	
	(b) Tunneling at Finite Temperatures.	40
FIGURE 5:	Multiparticle Tunneling.	41
FIGURE 6:	A Possible Quasiparticle Energy Diagram for a Two Band Superconductor.	42
FIGURE 7:	Tunneling in a Two Band Superconductor.	43
FIGURE 8:	(a) Josephson Effect	
	(b) Excitation of Quasiparticles by Absorption of Photons or Phonons.	
	(c) Photon or Phonon Assisted Tunneling.	44
FIGURE 9:	Test Sample Mounted for the Helium-3 Cryostat.	45
FIGURE 10:	(a) A Shorted Niobium-Indium Tunnel Junction.	
	(b) The Derivative of Figure 10a.	46
FIGURE 11:	(a) The Same Junction as in Figure 10 but with a Better Oxide.	
	(b) As in (a), but at 1.17K	47
FIGURE 12:	Structure in a Niobium-Indium Tunnel Junction at 0.48K.	48
FIGURE 13:	Type I Lead Junction.	49
FIGURE 14:	Type II Lead Junction.	50
	(a) Derivative of a typical junction.	
	(b) Type II junction showing a broadened sum peak.	

LIST OF FIGURES (con't)

FIGURE 15:	(a) Circuit Diagram of the Voltage Sources.	
	(b) Detection Network.	51
FIGURE 16:	Equivalent Circuits	52
	(a) D.C. Network	
	(b) A.C. Network	
FIGURE 17:	The Helium-3 Gas Handling System.	53

ACKNOWLEDGEMENTS

The author wishes to thank Professor R.M. Rose for enough rope and a good sense of humor for the duration.

He is most grateful for the technical expertise of Mr. I.M. Puffer especially for the construction of the cryostat and advice on almost everything.

Special thanks to Dr. M.L.A. MacVicar for highly stimulating discussions, and to Miss Carolyn Koehler for patience.

Finally, the warmest appreciation for Dr. John Wulff for "keeping the faith."

This research was supported by the Office of Naval Research.
Contract Number: NONR 3963(16).

INTRODUCTION

There is intense interest in high field, high temperature superconductors. A large number of superconductors having these properties are transition metals or compounds. The enhanced superconducting properties of these materials is believed to be intimately associated with their energy band structure. The overlapping of the s and d energy bands at the Fermi level leads to the intriguing possibility of two (or more) energy gaps in transition metals. The most satisfying direct experimental determinations of possible multigap existence and Fermi surface topology are obtained by sampling the excitation spectrum of a superconductor by electron tunneling across an insulating barrier.

The recent work of MacVicar¹ on the energy gap anisotropy in single crystal niobium also produced a wealth of data at low voltages which were unexplainable. The present work investigates that structure in detail to ascertain the existence of a possible second energy gap in niobium.

We shall first introduce the electron tunneling concept and expand the theoretical description. The nature of a second energy gap will be explored. We then discuss the possible structure observable at low voltages in the light of tunneling theory. The experimental approach is described along with a discussion of the insulating barrier. Results are presented along with further considerations on sources of low voltage structure. A discussion of the results follows along with the conclusions.

AN INTRODUCTION TO TUNNELING

In 1960, Giaever² observed that if two superconductors were separated by a thin insulating barrier a current would flow between them as a function of the voltage applied to the sandwich. The mechanism of current flow between these superconductors was electron tunneling, and we shall review here the basic concepts involved in this process.

We consider a superconductor as consisting simultaneously of correlated electron pairs (Cooper pairs)³ and "normal", unpaired electrons (quasiparticles). By "normal" we mean they behave analogously to electrons in a normal metal. At temperatures below T_c , some electrons form pairs and an energy gap appears in the quasiparticle excitation spectrum. This energy gap, denoted by 2Δ , corresponds to the binding energy of the Cooper pairs. Hence, if an energy 2Δ is supplied to a superconductor, pairs may become unbound.

Suppose we now separate two identical superconductors by an insulating barrier. The superconductors are assumed to be weakly coupled across the barrier and one may then consider the wavefunctions in each as independent of the other. If a bias voltage is applied at a temperature above T_c , one observes a linear current associated with the usual electron tunneling. Well below T_c , no current is observed until energy sufficient to create quasiparticles is supplied ($eV = 2\Delta$). At this point, a sharp current rise occurs and, for higher voltages, normal tunneling processes are observed.

If the barrier is quite thin, the pair wavefunctions in each superconductor will be coupled, differing only in phase across the boundary. As they are coherent over a sizeable range, this leads to the Josephson effect⁴

Tunneling may be used to investigate a number of properties of superconductors. Considering only the basic BCS⁵ theory of superconductivity, we find that there is a sharp increase in the quasiparticles density of states at the gap edge (infinite at $T=0$). If one uses two different superconductors, the gap edge in each acts as a fine probe of the excitation spectrum of the other. Also, as the tunnel junction supposedly samples electrons from a very small region moving perpendicular to the barrier⁶, we have an excellent probe to determine the energy gap as a function of position on the Fermi surface in single crystals (the energy gap is centered at the Fermi energy).

Most tunneling work has been done on sandwiches of thin films separated by an oxide layer owing to the relative ease of film fabrication. However, the data obtained from the films must yield only averaged values and involve microstructures rich in defects and disorder. Tunneling into single crystals is far more useful in determining the effects of Fermi surface topology and energy band structure on the energy gap and quasiparticle spectrum.

The fabrication of a single crystal tunnel junction is, at best, difficult and has met with little success in the past. Zavaritski⁷ has studied tin crystals and been able to determine the anisotropy of

the gap in k-space. Dietrich⁸ met with limited success in tunneling experiments on tantalum. Recently, MacVicar¹ has successfully formed junctions on pure single crystal niobium and determined the anisotropy of the energy gap using indium as the second superconductor.

ELECTRON TUNNELING REVISITED

As we shall use the Schrieffer excitation representation⁹ for electron tunneling in the discussion of our results, we present here the theory of various tunneling processes.

The conventional semiconductor model as introduced by Nicol, et al¹⁰, tends to be misleading in that the model implies single particle states both above and below the energy gap with momentum $k > k_f$ above the gap and $k < k_f$ below the gap. Further, one cannot as in a semiconductor, inject particles into an empty band without disturbing the full band: hole or electron-like excitations have no real meaning since an excitation of a superconductor is defined only as the presence of an uncondensed electron. Since each uncondensed electron renders a pair of k states inaccessible to the superfluid, the energy of the system is raised. Hence, to create an excitation, we must add energy to the entire system. We shall consider this energy as being carried by the excitation. Viewing the excitations in this manner also allows for the condensation of two electrons (or holes) into a pair at the chemical potential.

Let us examine the excitations of a superconductor more closely and consider the quasiparticle excitation energy plotted against momentum as shown in figure 1. The expression for the single quasiparticle energy relative to the chemical potential (Fermi energy) is:

$$E_k = (\epsilon_k^2 + \Delta_k^2)^{1/2}$$

where ϵ_k is the Bloch energy of an electron in the normal state relative to the Fermi energy⁹. Note that at the Fermi energy ϵ_k is zero and the excitation energy per particle is Δ , the gap parameter.

We now consider a single particle tunneling process between two superconductors A and B. (see figure 2). An electron from a condensed pair located at E_f (recall that we have defined our zero of energy at the Fermi energy) in superconductor A is placed at $E_{k_1}^A$ and the other member of the pair tunnels through the barrier to the excited state $E_{k_2}^B$ in superconductor B. To conserve energy, a bias voltage of $eV = E_{k_1}^A + E_{k_2}^B \geq \Delta_A + \Delta_B$ must be applied. The sole effect of the bias voltage is to shift the relative position of the chemical potentials; the tunneling process itself always involves a net energy change of zero. It should also be noted that all values of k both above and below k_f are potentially available to an excited electron even at absolute zero temperature. This is not obvious on the semiconductor model.

We shall simplify the excitation diagrams by noting that the current onset for single particle tunneling is at $eV = \Delta_A + \Delta_B$. For our purposes, we need only consider the biases at which current flow is initiated and accordingly we shall draw the diagrams only at the minimum energy of excitation as shown in figure 3. for the case of single particle tunneling. A temperature dependent process is shown in figure 4. The density of states for quasiparticles is shown above the gap only. The probability of occupation of the quasiparticles is shown above the gap only. The probability of occupa-

tion of the quasiparticles energy above the gap is simply given by the Fermi function as shown. When a bias voltage is applied, the chemical potentials are shifted by an amount $eV = \Delta_A - \Delta_B$ at the current onset as seen in figure 4b. This is the origin of the "difference" peak in the I vs V characteristic for tunneling between two different superconductors.

The amount of current flowing through the barrier by a tunneling process depends both on the number of states occupied by quasiparticles on one side of the barrier and the availability of states on the other side. Needless to say, the superconducting density of states will determine the tunneling current and, in fact, by measuring the change in current with voltage (the derivative of the current vs voltage trace) one scans the density of the states.

MULTIPLE BAND SUPERCONDUCTIVITY

In 1965, Shen, et al¹¹ reported specific heat measurements on niobium yielding values significantly larger than predicted by the BCS theory for temperatures lower than $T_c/10$. They were unable to use the anisotropy of the energy gap to explain their results and postulated the existence of a second energy gap at an energy $\Delta/10$ ¹². It is noteworthy that Shen's experiments were done on a low purity (resistivity ratio 110) single crystal of niobium and on a polycrystalline sample. The latter showed less of a deviation in C_v .

Shen's conclusions were based on the ideas of Suhl, Matthias and Walker (SMW)¹³. The BCS theory was extended directly to the case of two energy bands, both with an attractive BCS-type interaction, incorporating interband pair scattering (by phonons). Using the same energy cutoffs for both bands, SMW found two quasiparticle excitation spectra and two gap parameters. With interband scattering, the superconductor was found to have two energy gaps but only one transition temperature. In the limit of no interband scatter, there would be two transition temperatures.

Kondo¹⁴ proposed an extension of the work of SMW by treating the second band, partially above the Fermi sea, as having a repulsive electron-electron interaction. The presence in this narrow band of a large density of states at the Fermi energy was found to enhance superconductivity when this band interacted with a band whose electrons behaved in the BCS manner. Two types

of pairs were considered (one for each band) and a repulsive interaction in the d band was assumed independent of electron-phonon effects. It was found that a pair in the s band (or conversely) is "virtually" excited (momentarily finds itself in the other band) then drops back into its own band. The resulting second order process appears as an attraction in the BCS band enhancing the transition temperature. The large density of states increases the phase space available for superconducting pair scatter. If these states are above the Fermi level, the pairing is no longer symmetric and changes in the chemical potential must be considered. Lanthanum, in particular, could exhibit this type of behavior.

Garland¹⁵ assumed that the Fermi surface was separable into s and d portions. For "clean", in the Anderson sense¹⁶, transition metals, two gaps are present and the following could contribute to the superconductivity of these metals: a) an attractive s-band coulomb interaction due to the presence of the d-electrons; b) BCS interactions for both bands; c) a Kondo-like interband coupling. For "dirty" transition metals, only one energy gap is found since the quasiparticles will have both s and d character by mixing due to impurity scatter. Noting the higher density of states for the d band, the superconductivity will be dominated by these electrons. Garland expects only one transition temperature in either case.

Peretti¹⁷ has demonstrated that, in general, an s-d interaction leads to superconductivity even if the interaction within each band is zero. Two gaps are found with one transition temperature.

Soda and Wada¹⁸ continued the discussion of the two band theory in their investigation of the specific heat of transition metals and alloys. They extended the model of SMW and considered only intraband pairing, coming to the following conclusions:

a) there will be two transition temperatures, one for each gap, if both bands have a BCS nature; b) if there is any interband coupling, only one transition temperature will be present but two gaps will persist to T_c ; c) one of the energy gaps will be larger than the BCS value of $3.5 kT_c$, the other will be very much smaller. A weighted average of the two gap values leads to the experimentally observed BCS value.

In discussing Shen's results, Soda and Wada suggest that at higher temperatures strong coupling effects may destroy the two gap phenomena. At lower temperatures, the damping of the quasi-particle excitations may become less of an influence and allow observation of the second gap.

To sum up the basic ideas of the theory of transition metal superconductors; two or more energy bands are assumed to lie close to each other at the Fermi energy and a BCS weak coupling approach may be applied separately to each band, giving rise to two energy gaps and two excitation spectra. Two transition temperatures will appear if there is no pair formation or scattering between bands. If there is any interband coupling present, one transition temperature but two gaps may exist. If electron pairs are scattered between the bands and one band has a large density of states, T_c is enhanced. If electron coupling between bands is quite strong, only one energy gap should exist¹⁹.

INTRODUCTION TO LOW VOLTAGE TUNNELING STRUCTURE

The structure corresponding to a second energy gap that may be found in tunneling curves will be expected to fall at rather low biases. In this same region, a great amount of other detail appears in tunneling data and is discussed here.

Below the sum peak in superconductor-superconductor tunneling, one expects very little current at temperatures well below the transition temperatures of the two superconductors. The small currents expected would be due to thermally excited quasiparticles. In practice, much larger currents are observed and these "excess currents" may exhibit low voltage structure. (Strictly Schottky phenomena would give rise to structureless excess currents which are very temperature dependent)

In addition to the obvious current peak at $\Delta_A - \Delta_B$, which is a thermal quasiparticle peak, peaks in the I-V curve at Δ_A and Δ_B are observed along with a series of peaks associated with $2\Delta_i/h$. The structure at Δ_A and Δ_B is called "multiparticle" tunneling²⁰ and, originally, was thought to be related to thin spots in the oxide barrier between the two superconductors. In an I-V characteristic showing this behavior, there is a large current increase in the vicinity of Δ_i . This increase is rather broad and very much smaller than the current jump at the sum peak. Thermal smearing or thermal phonons appear not to contribute to the width of the current rise²¹. The mechanism of this process as proposed in reference 20, is the tunneling of both members of a pair in one superconductor into the other, appearing there as

excitations. The process is second order, hence the proposal of thin oxides was necessary to account for the magnitude of the currents observed. The fact of a broad current onset suggests a more complicated mechanism²¹.

Subharmonic structure (SHS)^{21,22,23,24} will appear at biases of $2\Delta/n$. SHS is an excess current increase superimposed on a slowly varying background current. It is almost always associated with junctions of exceptionally low resistances (less than 1 ohm) which show large Josephson currents or shorts. The position of the SHS exactly follows the temperature dependence of the peak at 2Δ ²⁴. In fact, any structure in the 2Δ peak is exactly reproduced in the SHS²². The mechanism of SHS is most certainly not similar to multiparticle tunneling²¹, but the exact nature of the processes involved are, at present, unknown. Rowell and Feldman²¹ believe that subharmonic behavior is not a true tunneling process and is independent of any other process going on in the junction. They believe that SHS arises from metallic bridges through the barrier. The possible mechanism for SHS are discussed elsewhere in the thesis.

The last type of low voltage structure arises from Josephson tunneling and oxide shorts. (The two may be distinguished by whether the curve is hysteretic through zero bias) When Josephson tunneling switches to the usual quasiparticle tunneling, it often does so in steps called Fiske modes²⁵. Oxide shorts, as they switch to normal links (supplying a linear background current), often exhibit current bursts. Both effects are readily distinguishable in the derivatives of the I-V curves.

THEORY OF LOW VOLTAGE TUNNELING STRUCTURE

It is possible to initiate a tunneling process at bias voltages of Δ_A and Δ_B as shown in figure 5. This so-called "multiparticle" tunneling process is a second order event and apparently dependent on the thickness of the oxide barrier²⁰. M-particle processes are possible, but they are of very high order on this model and are highly unlikely. By high order, we mean powers of the tunneling matrix $|T|$ where $|T|$ is obtained by analogy with the classic WKB treatment of quantum mechanical tunneling. The single particle current contains a factor $|T|^2$ and any M-particle process would contain a factor $|T|^{2M}$. The M-particle event would initiate at biases Δ_A/M and Δ_B/M .

Let us now consider a quasiparticle energy diagram for a multiband superconductor as displayed in figure 6. Note that the zero of energy is the same for all condensed pairs coming from different bands lying at the Fermi energy in the normal state. (This is not meant to imply that the ground state energy is the same for each type of pair.) There will, however, be a different excitation spectrum for each type of pair. Tunneling currents between the two band superconductor and a one gap superconductor may initiate at bias voltages of $eV = \Delta_a; \Delta_b; \Delta_a - \Delta_a; \Delta_b - \Delta_a; \frac{\Delta_a + \Delta_b}{2}; \Delta_a + \Delta_b$ and $\Delta_a + \Delta_a$. All the peaks are obtainable by examining previous diagrams except $\frac{\Delta_a + \Delta_b}{2}$ which is shown in figure 7. We assume no interband transitions.

As it is difficult to justify higher order multiparticle tunneling processes beyond $\frac{2\Delta}{2}$, we must search for other mechanisms to explain structure regularly observed at very low voltages. As SHS is generally observed in junctions with thin barriers we consider processes requiring these barriers.

Josephson tunneling (figure 8a) will occur through thin barriers and generate an ac current at a finite bias. An ac field will be present in the junction along with its harmonics at frequencies²⁶:

$$\omega = 2neV/\hbar$$

where n is the harmonic number. We note in passing that power is also supplied to the junction at 2neV by shorts present in the oxide²⁷.

The ac field can be absorbed by the superconductors on either side of the junction, creating quasiparticles in both as shown in figure 8b. This will occur at $n \cdot 2eV \geq 2\Delta_A$ or $2\Delta_B$, giving an even series of current peaks at:

$$eV = 2\Delta_i/2n$$

The radiation present in the junction can also interact with the single particle tunneling current, as in figure 8c, to yield an odd series of current steps at:

$$eV = \Delta_A + \Delta_B / 1 + 2n$$

A single particle, upon absorption of a photon, will tunnel when its energy plus the photon energy is equal to $\Delta_A + \Delta_B$: that is when $eV + \hbar\omega = \Delta_A + \Delta_B$.

Interaction of the radiation with higher order processes is possible but it would be difficult to detect.

General Considerations:

To observe finely detailed, low voltage structure in a tunnel junction we must first select a fine probe. In our case, a thick indium film ($T_c = 3.4K$) is used as it has one sharp, well-defined energy gap. (Other gaps have been reported⁴⁶, but they were not observed in this experiment.) The indium gap value is small compared to niobium (9.2K) enabling easy separation of the peaks in the tunneling data, yet large enough to minimize thermal smearing of the gap edge at the temperatures used in these experiments. Indium films withstand thermal cycling and are chemically stable thus enabling repetition of experiments.

Very pure niobium single crystals are needed for several reasons: the observation of a second energy gap may depend on interband coupling via impurities, any anisotropy of tunneling structure may be washed out by impurities¹⁶, surface impurities or imperfection may introduce additional low voltage structure.²¹

Low temperatures are required to minimize excess currents, sharpen the gap edges (the sensitivity of the technique depends on the absence of thermally excited quasiparticles), and to determine the existence, if any of an additional transition temperature for a possible second gap.

Resolution of current peaks (tunneling events) often not visible in a current versus voltage plot requires the use of derivative techniques as described in the appendix. A current peak is simply a change

in conductance across the junction; the derivative, dI/dV , will exhibit a peak at each conductance change.

Procedure:

Niobium single crystals are grown in vacua of 10^{-9} Torr by the electron beam floating zone technique from 1/8" diameter polycrystalline rod seeded to the desired orientation. Traverses of the rod are made rapidly, at the expense of some crystal perfection, to reduce recontamination from the vacuum. Several crystals of exceptional purity were grown from niobium electrodeposited from fused salts³⁷. The average resistivity ratio for niobium grown from the rod was 400 (uncorrected for magnetoresistance) while two crystals of the special purity niobium had ratios of 1300 and 3300. The samples used in our experiments were certainly above the "clean" superconductor level^{1,16}.

After cooling, the single crystal rod is sectioned to the required length and oxidized by glow discharge. The crystal sections are placed at the center of a niobium cylinder which is at negative potential with respect to the crystals. A constant oxygen pressure of 150 microns is maintained by a variable leak. The glow is maintained for 16 minutes. Samples oxidized by this method show junction resistances of between 50 and 100 ohms.

The samples are now masked with formvar for electrical contact placement and narrow indium or lead stripes of about 4000 Angstrom thickness are evaporated at the desired niobium crystallographic orientation. Thickness is estimated from evaporation rate of 100 to 200 Angstroms per second. Care is taken to maintain the pressure during evaporation at such a point that the indium forms a continuous

amorphous film. (Some oxygen contamination is required to prevent the indium films from forming islands.)

Electrical contact to the junctions is made by two current and two voltage leads using 5 mil gold wire. A current and voltage lead is connected to each side of the junction with flexible silver paint capable of being thermally cycled. Figure 9 shows such a junction.

The samples are then cooled to as low as 0.5K in a helium-3 cryostat and I - V characteristics and their derivatives taken as described in the appendix.

CONSIDERATIONS ON THE INSULATING BARRIER

Detailed knowledge of the oxides of niobium, their formation and growth is sadly lacking. Niobium oxide growth apparently occurs by migration of niobium atoms to the oxide-gas interface. The initial oxide is amorphous when grown thermally, but in time forms suboxides and becomes polycrystalline. Growth becomes much more rapid as diffusion can take place along boundaries and the oxide breaks away from the surface²⁸.

Niobium oxidized at 125° C for about 45 minutes is found to exhibit low resistance, but non-shorting behavior when used as a tunneling barrier¹. Niobium oxidized by glow discharge at the edge of the glow region for 16 minutes at a pressure of 150 microns of oxygen frequently exhibits shorting behavior and ten times the junction resistance compared to the thermally oxidized samples. The effective temperature at the surface of the niobium during the glow discharge cannot be determined, but it is likely substantially higher than 100° C by the junction resistance standard alone. The glow discharge oxide is likely much thicker than a thermally grown oxide.

The thermally grown oxide is most likely amorphous and quite thin²⁸ or, remotely, epitaxial²⁹. The glow discharge oxide exhibits polycrystalline behavior with a multitude of suboxides present^{30,31}. This is supported in the tunneling data by the presence of shorts and the fact that after a week on the shelf, some junctions "healed" and no longer exhibited shorted behavior suggesting surface diffusion. Larger background currents are consistently observed in

these junctions as opposed to the thermally grown oxides, suggesting that there are alternative conduction paths through the oxide. The barriers formed by glow discharge could also contain metallic impurities sputtered off the other electrodes.

The Niobium-Oxide Interface:

The as-grown niobium single crystal exhibits a very smooth surface free of sizeable pits due to thermal etching³². Slowly grown or annealed specimens show more etching and prove to be of poorer quality for tunneling experiments. These local areas of imperfection may cause thin spots in the amorphous oxide leading to low voltage breakdown or Josephson effects. The internal surfaces of a thermal etch pit are low energy surfaces and probably retard oxide growth.

It may be important to know how the composition of the oxide is altered in the transition from pure niobium to the oxide mixture containing various suboxides (Nb_2O_5 , NbO , NbO_2). The transition layer at the interface could alter the energy gap by proximity effects³³ or modify the coupling of the superconducting wave functions at the boundary^{34,35}.

It is unlikely that an interface layer of substantial thickness could be built up under our conditions of fabrication. Diffusion of oxygen into niobium at the temperatures of the oxidation procedure is negligible³⁶ as is the adsorbed layer formed during crystal growth in high vacuum. Surface segregation of non-volatile impurities is unlikely. Surface contamination is further hindered

by back-filling with oxygen before removing the crystal from the vacuum chamber. At best, the interface layer is of the order of tens of Angstroms while the total oxide layer is probably less than 100 Angstroms.

We present here a summary of information drawn from the data of niobium-oxide-(lead or indium) tunnel junctions. We observe, in addition to the usual sum and multiparticle peaks, some subharmonic structure and very low voltage structure which is apparently not related to subharmonic phenomena. Examples of the data are presented in figures 10 through 14.

The data from lead must be sorted into two different classes: that taken from junctions showing no sum peaks and very broad multiparticle peaks (if any), and that taken from junctions exhibiting both sum and multiparticle peaks. We shall refer to these classes as type I and II respectively. See figures 13 and 14.

Type I junctions differ from type II only in the manner of oxide formation: Type I was oxidized by glow discharge and exhibited junction resistances of several hundred ohms; type II was thermally oxidized in a stream of oxygen at a temperature of 125°C for 45 minutes and was found to have a junction resistance of 3 ohms.

Type I junctions show large background currents but no evidence of current shorts. Type II junctions showed considerably less background current and no shorts of Josephson behavior. Both types, however, exhibit a great deal of sharp low voltage structures which is temperature dependent. This temperature dependent structure is not observed in junctions formed with indium, although similar structure may be found in the data of MacVicar¹. The temperature dependence and the intensity of the peaks suggests that the low voltage structures in the lead junctions is not SHS.

Junctions formed with indium often exhibit an extra peak at very low voltage with no apparent temperature dependence in the range 4.2K to 0.45K. The orientation of these junctions is predominately $\langle 111 \rangle$ and $\langle 110 \rangle$. The peaks also appear at the same orientations in the data of MacVicar¹ which suggests that they are independent of the nature of oxide formation. They also exhibit possible sum and difference peaks with other structure. For example, in the indium data (Figures 11 and 12) some structure is observed near the multiparticle peak which may indicate the presence of a gap near $0.15 (10^{-3} \text{eV})$. Another temperature independent peak appears at half the value of the peak near 0.15 meV.

FURTHER CONSIDERATIONS ON THE SOURCES OF
LOW VOLTAGE TUNNELING STRUCTURE

Subharmonics:

Subharmonics structure is discussed in a previous section and is only briefly reviewed here. It should be pointed out that the effect is not at all understood. Structure is seen in the tunneling data at values $2\Delta/n$ with n an integer. It is generally associated with a large background current and shorted junctions. (The background current may come from tunneling processes as well as the shorts.) Zero bias anomalies are generally present. The structure is temperature independent except for the dependence of Δ on T and is most evident in demonstrably thin oxide barriers.

The current displayed in a SHS peak is found to be related to the current at the 2Δ peak by the ratio $I_{2\Delta}/n$ and the maximum current at peak n is twice that seen at peak $n+1$ ²².

Marcus²³ believes that SHS originates at minute metallic shorts in the barrier that have been driven normal by the tunneling current. It is perhaps possible that the structure arises from small particles within the oxide not shorted to either side. (See later discussion).

Lastly, we point out that if the mechanism of SHS involves Josephson tunneling processes, then the superconductor with the smallest energy gap should display the stronger SHS. This is simply due to the fact that lower harmonics of the ac field are required.

Multiparticle Processes:

Multiparticle tunneling was originally believed²⁰ to be higher

order processes requiring thin oxides for observability and some evidence supports this approach. However, the onset of current at Δ apparently is somewhat broad (see figure 11) and it has been suggested that a collective excitation of the condensed state may occur at energies somewhat less than Δ ²¹. If it is an excited state of a pair, then two quasiparticles must be injected to observe it thereby yielding a peak near $\frac{2\Delta}{2}$.

Fundamental Josephson or Short Behavior:

Excitation of Josephson modes or the presence of resistive shorts produces current steps at very low biases and is readily identifiable in the I-V plots (see figure 10). Large background currents are characteristic of such junctions as may be seen by comparing figures 10 and 11.

The Presence of a Contributing Barrier:

An interesting conjecture is the possibility that the interface between the pure niobium and its oxide may contain metal-rich oxides in the form of islands or as a weakly superconducting or normal layer (NbO is in fact a superconductor with a transition temperature of about 1 K).

The origin of this layer could be by the sputtering of impurities into the oxide layer during glow discharge, local growth of the oxide layer at surface irregularities or by the contamination from the vacuum in which the crystal was grown. Low voltage structure appears more commonly in oxides deposited by glow discharge. These oxides are fairly thick and most likely polycrystalline as discussed earlier. The conditions under which the oxidation was performed could easily

introduce metallic impurities.

Small islands of weakly superconducting material imbedded in the oxide could give a series of low energy structure. Indeed, Giaever³⁸ has observed superconductivity in particles smaller than 25 Å in diameter imbedded in the insulating layer of a tunneling junction. As the particles get smaller, their transition temperature rises.

A layer or cluster of normal material near the crystal-oxide interface could also be superconducting by virtue of the proximity effect and exhibit an energy gap somewhat less than the niobium gap depending on the thickness of this normal layer⁴³. The effect would show up as a broadening of the niobium peak and the sum peak.

Often one sees a sharp dip in the density of states near the sum peak¹ (see figure 11) possibly as a result of quasiparticle interference (eg. reflection) in the normal surface layer³⁹.

The value of the energy gap in a normal region is open to some speculation since the details of that layer are unknown. The value of the interaction parameter ($N(0)V$) may change radically at the interface (within a few Å into the oxide) due to the dissimilarity in the phonon modes between the oxide and the crystal⁴³. This could perhaps lead to an apparent T_c .

Localized excitations may possibly be detected from within the normal layer⁴³. A high density of states is present in the normal-metal side of a proximity layer and exhibits gaplessness (zero bias conductance) only for thick layers²¹.

The same events could occur at the film-oxide interface: especially for lead junctions. Here, in addition to the niobium oxide, there is the possibility of lead rich oxides. Also, the lead film certainly

does not make smooth contact with the oxide and the rough surface could give unknown interference effects.

DISCUSSION

We consider first the low voltage structure in the lead junctions. The first conclusion would be that it is SHS and, indeed, the values of the various peaks are close to that of anticipated SHS. In the following discussion, we present evidence that the low voltage structure is not SHS.

Considering the position of the peaks, SHS would exhibit a series of current peaks whose spacing would decrease rapidly with increasing n . Further, the temperature dependence of the peaks is expected to identically match that of the gap from which they are derived²⁴. Neither of these requirements are met in either type I or II junctions.

The intensity of the current peak is stronger than one would anticipate for higher order SHS and it does not drop off as $1/n$, as expected. The current ratios between neighboring peaks does not agree with Marcus' results²².

One lead junction had particularly broad film edges. The I-V and derivative curves show a broadening at the sum peak indicative of multiple energy gaps in the lead film (see figure 14c). No change occurs in the low voltage structure. We suggest that this low voltage structure is not the SHS of multiple lead energy gaps as in the data of Rochlin⁴⁴.

There is no visible evidence for shorting (considered essential for SHS) in either type I or II junctions although we do observe a zero bias anomaly in the derivatives. Strangely

enough, no structure is observed in a junction on the same crystal which is suspected of containing a short.

What is observed, is indications that the source of low voltage detail is within the barrier. Consider the peak at 0.62 meV in figure 14. It appears to form a sum peak with both the lead and niobium multiparticle peaks and it maintains the correct position(s) with an increase in temperature. The remaining low voltage peaks exhibit temperature dependencies which appear to preclude their being SHS.

We must, of course, consider the possibility that the structure is indeed SHS or related to SHS. Non-shortcd junctions have, on occasion exhibited SHS, although the evidence is not clear^{23,24}. Also, there is claim that SHS is observed in junctions not exhibiting all the usual processes such as single particle tunneling^{23,24}. Again, the evidence is somewhat tenuous. We also note that SHS is observed only (so far) in junctions formed by oxidizing one of the members. Our type I junctions, which are probably heavily oxidized, show the strongest low voltage structure. These junctions were also pre-cooled in liquid nitrogen before insertion into the liquid helium. The process of transferring the sample from one dewar to another could result in severe damage to the lead film (effectively changing the barrier) by oxidation with the liquid oxygen condensed on the sample. (The type II junctions were immersed directly into the liquid helium.)

We propose that if we are seeing SHS, then the mechanism lies within the oxide barrier as the process can be altered somewhat by changing the oxide characteristic. If the source

arose from small particles imbedded within the oxide or by proximity effects as the presence of a zero bias anomaly suggests, then one could possibly observe an "apparent" transition temperature. This might also explain Rowell's comment that the "gap" given by $\frac{2\Delta}{k} \cdot n$ progressively decreases as n is increased. Something similar to this is observed in type I junctions.

MácVicar¹⁵ has suggested that there may be facets on the surface of the niobium which become field emitters. (the tunnel junction will develop very high voltages at small points). Field emission would give a temperature dependent exponentially increasing background current. Different points on the surface could have different thresholds for emission. The result would be an increasing (with voltage) background current with current bumps at each threshold voltage. SHS fits this description²².

We must state that the peaks in figure 14 located at 0.62 meV, 0.50 meV and 0.35 meV fit, at first glance, a niobium SHS series for $n= 5,6$ and 9 . However, the peak at 0.62 meV must originate within the oxide as it forms a sum peak with both members of the junction. (There could be a difference peak at 0.90 meV). The temperature dependence of the other peaks is incorrect for SHS as it suggests a transition temperature less than either that of lead or niobium. The temperature dependence could be non-BCS which would seem to rule out SHS. We do not have enough points to determine the nature of the temperature dependence.

More interesting are the temperature independent peaks in the indium junctions and the fact that they appear predominately in junction oriented near $\langle 111 \rangle$ and $\langle 110 \rangle$. The structure

does not appear to be part of a series and there are indications of other tunneling events involving this peak. These events often appear as structure in or near the indium multiparticle peak. (see figures 11 and 12)

The lack of temperature dependence precludes the peaks from being related to the indium gap (the peak at 0.24 meV is a SHS). The invariance of the peak over such a wide temperature range prevents it from being either a niobium subharmonic or a gap arising from a superconducting impurity in the oxide.

It is tempting to identify structure in the lead junctions as arising from the interactions of this new peak with low voltage structure in the barrier. Although no evidence of sum and difference peaks involving SHS has, to date, been reported, there is no reason to not expect such behavior from structure originating within the barrier. Considering the data of figure 14, we note structure in the derivative at 0.35 meV indicative of a difference peak. (the resonance-like structure is characteristic of difference peaks). The sum peak would appear at 0.65 meV but might be obscured by the peak at 0.62 meV. We note that the apparent "difference" peak sharpens with increasing temperature, as would be expected, and maintains a constant distance (0.15 meV) from the temperature varying peak at 0.50 meV.

Although the peak at 0.15 meV will appear in a shorted junction, the evidence suggests that it is not related to shorting behavior. It is obscured by the presence of excess currents and is independent of the amount of current flowing through the junction. When all evidence of shorted behavior is removed, as shown in figures 10

and 11, the peak remains. The junction resistance was increased in this case from 4 to 160 ohms. Surely the breakdown voltage for this junction was significantly increased.

We suggest that the current peak near 0.15 meV arises from a second energy gap indicating a second superconducting energy band in niobium. The value of the peak agrees well with the theoretically predicted value of $\Delta/10$ ¹². A temperature dependence is not required of a second gap as the interaction causing it may depend only on the presence of other superconducting electrons; for example in a nearby d band. If the proximity of another band of electrons is required, the best directions in niobium are $\langle 111 \rangle$ and $\langle 110 \rangle$ ⁴⁰.

The appearance of the peak in the $\langle 100 \rangle$ direction (infrequently) may simply be due to the inability to reduce the angle subtended by the film on the Fermi surface to sample only $\langle 100 \rangle$ sections. Also, the oxide film may be so oriented that it selects several different orientations of the Fermi surface³⁴. Most simply, the second energy gap may be truly isotropic. The gap has appeared in an insufficient number of junctions to truly test the anisotropy.

Laibowitz⁴¹ has found structure at $\Delta/10$ in niobium thin films oxidized by anodization. The structure also has a non-BCS dependence on temperature. Forgan, also, has apparently found evidence for a second gap in acoustic attenuation experiments⁴².

CONCLUSIONS

We have studied the tunneling characteristics of niobium single crystals using lead and indium as the second superconductor. We have found low voltage structure in both types of junctions.

For the lead junctions, we find low voltage structure which does not easily fit the concept of SHS. We conclude that it originates within the oxide barrier. No conclusive statement may be made concerning this structure other than the fact that at least one of the peaks interacts with both the lead and niobium gap.

As the low voltage structure in lead junctions resembles SHS, we surmise that SHS may result from barrier impurities and instabilities. Metallic impurities or surfaces within the barrier may become breakdown sites. The large background current in glow discharge oxides could be due to conduction paths through the impurities or originate at imperfections.

We have evidence, primarily from the indium junctions, that a second energy gap occurs in niobium with a value $\Delta/10$ in agreement with theory. The behavior of this gap is consistent with that expected of an energy band in close proximity to another, more heavily populated, band. We have not confirmed any anisotropy of this gap, if any indeed exists.

SUGGESTIONS FOR FURTHER INVESTIGATION

As in anything else, a little bit of insight brings a great deal of unanswered problems. We suggest the following items be pursued:

1. Further studies on the anisotropy of the low voltage structure in niobium.
2. Fermi surface correlation of both niobium gaps and matching with phonon data.
3. Fabrication of non-oxide tunneling barriers on single crystals.
4. Search for SHS in non-oxide barriers.
5. Density of states measurements on SHS.
6. Tunneling exploration of possible collective excitations of the superconducting state.
7. Determination of oxide structure by LEED.
8. A study of the surfaces involved in a tunnel junction.
9. Extension of the search for multiple gaps to other transition metals.

REFERENCES

1. M.L.A. MacVicar, Sc.D Thesis, (1967), M.I.T. Department of Metallurgy.
2. I. Giaever, Physical Review Letters, 5, 147, 464, (1960).
3. L.N. Cooper, Physical Review, 104, 1189, (1956).
4. B.D. Josephson, Advances in Physics, 14, 470, (1965).
5. J. Bardeen, L.N. Cooper, and J.R. Schrieffer, Physical Review, 108, 1175, (1957).
6. W.A. Harrison, Physical Review, 123, 85, (1961).
7. N.V. Zavaritsky, Soviet Physics JETP, 18, 1260, (1964);21, 557, (1965).
8. I. Dietrich, LT8, ed. by R.O. Davies, Butterworths Pub., Washington,D.C., 173, (1963).
9. J.R. Schrieffer, Reviews of Modern Physics,36, 200, (1964).
10. S. Shapiro, et al, IBM Journal, January,1964, p.34.
11. L.Y.L. Shen, N.M. Senozan, and N.E. Phillips, Physical Review Letters, 14, 1025, (1965).
12. C.C. Sung, and L.Y.L. Shen, Physics Letters, 19, 101, (1965).
13. H. Suhl, B.T. Matthias, and L.R. Walker, Physical Review Letters, 3, 552, (1959).
14. J. Kondo, Progress of Theoretical Physics, 29, 1, (1963).
15. J.W. Garland, Physical Review Letters, 11, 111, (1963).
16. P.W. Anderson, Journal of Physics and Chemistry of Solids, 11, 26, (1959).
17. J. Peretti, Physics Letters, 2, 275, (1962).
18. T. Soda and Y. Wada, Progress of Theoretical Physics, 36, 1111, (1966).
19. W.S. Chow, Physical Review, 172, 467, (1968).

20. J.R. Schrieffer and J.W. Wilkins, Physical Review Letters, 10, 17, (1963).
21. J.M. Rowell and W.L. Feldman, Physical Review, 172, 393, (1968).
22. S.M. Marcus, Physics Letters, 19, 623, (1966).
23. S.M. Marcus, Physics Letters, 20, 236, (1966).
24. A.A. Bright and J.R. Merrill, to be published in Physics Review.
25. M.D. Fiske, Reviews of Modern Physics, 36, 221, (1964).
26. B.D. Josephson, Review of Modern Physics, 36, 216, (1964).
27. P.W. Anderson and A.H. Dayem, Physical Review Letters, 13, 195, (1964).
28. J. Harvey and P.H.G. Draper, Journal of the Institute of Metals, 92, 136, (1964).
29. D. Shoemaker, Private Communication.
30. W. Schroen, Journal of Applied Physics, 39, 2671, (1968).
31. J. Nordman, Journal of Applied Physics, 40, 2111, (1969).
32. D.D. Morrison, Private Communication.
33. P.G. deGennes, Reviews of Modern Physics, 36, 225, (1964).
34. J. Dowman, M. MacVicar, and J. Waldrum, To be published in Physical Review.
35. H. Prothero, Private Communication.
36. K.A. Jones, Ph.D. Thesis (1968) M.I.T. Department of Metallurgy.
37. Provided by R.W. Meyerhoff
38. H.R. Zeller and J. Giaever, Physical Review, 181, 789, (1969).
39. S.M. Freake and C.J. Adkins, Physical Letters, 29A, 382, (1969).
40. L.F. Mattheiss, Physical Review, 139, A1893, (1965).
41. R. Laibowitz, Private Communication.
42. E. Forgan, Private Communication.
43. C.J. Adkins and B.W. Kington, Philosophical Magazine, 10, 971, (1966).

44. G.I. Rochlin, Physical Review , 153, 513, (1967).
45. M.L.A. MacVicar, Private Communication.
46. T.D. Clark, Physics Letters, 27A, 608, (1968).

FIGURE 1: Quasiparticle Energy Verses Wavenumber

The minimum is at k_f where $\epsilon_{k_f} = 0$.

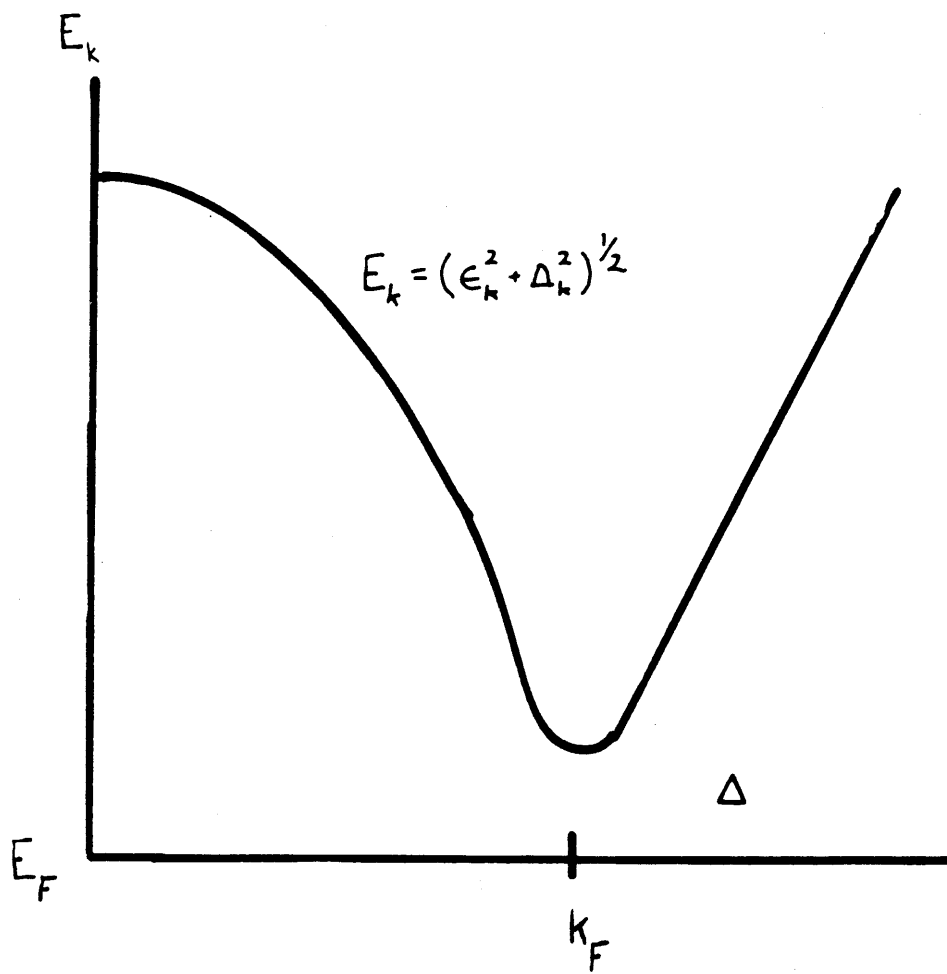


FIGURE 2: Single Particle Tunneling

$$eV = E_{k_1}^A + E_{k_2}^B \geq \Delta_A + \Delta_B$$

(After Schrieffer ⁹)

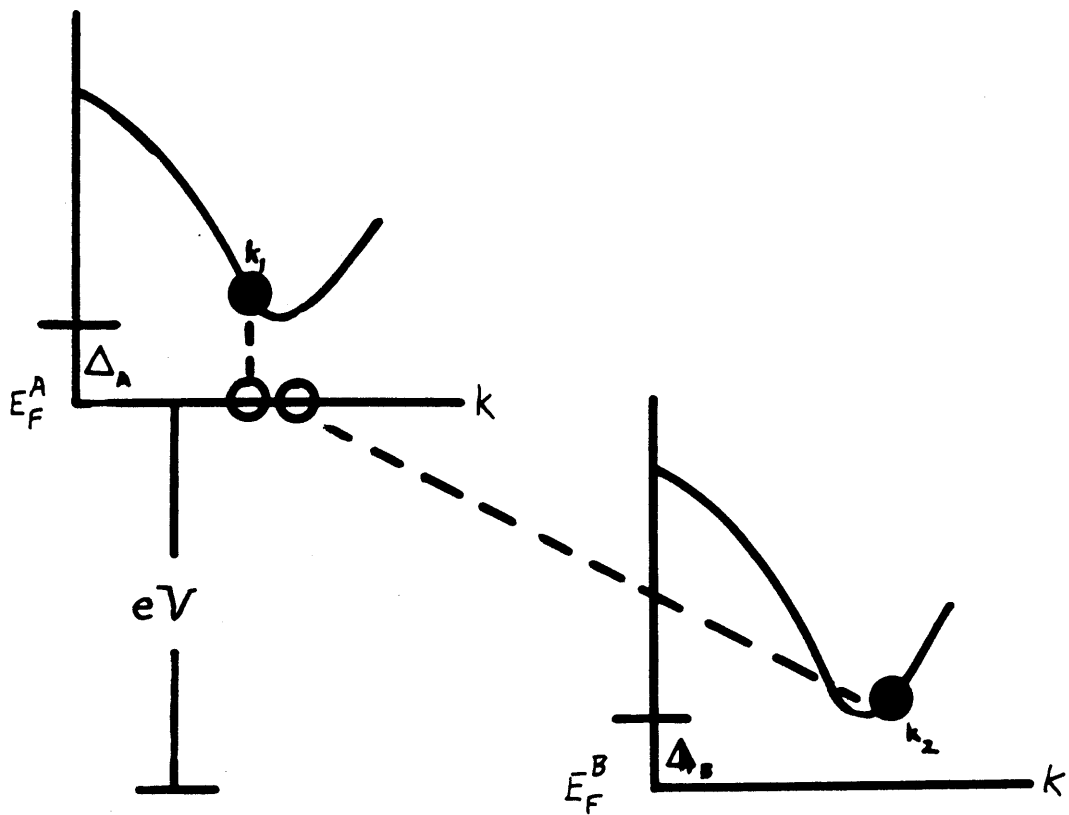


FIGURE 3: Minimum Energy Diagram for the Process Illustrated
in Figure 2.

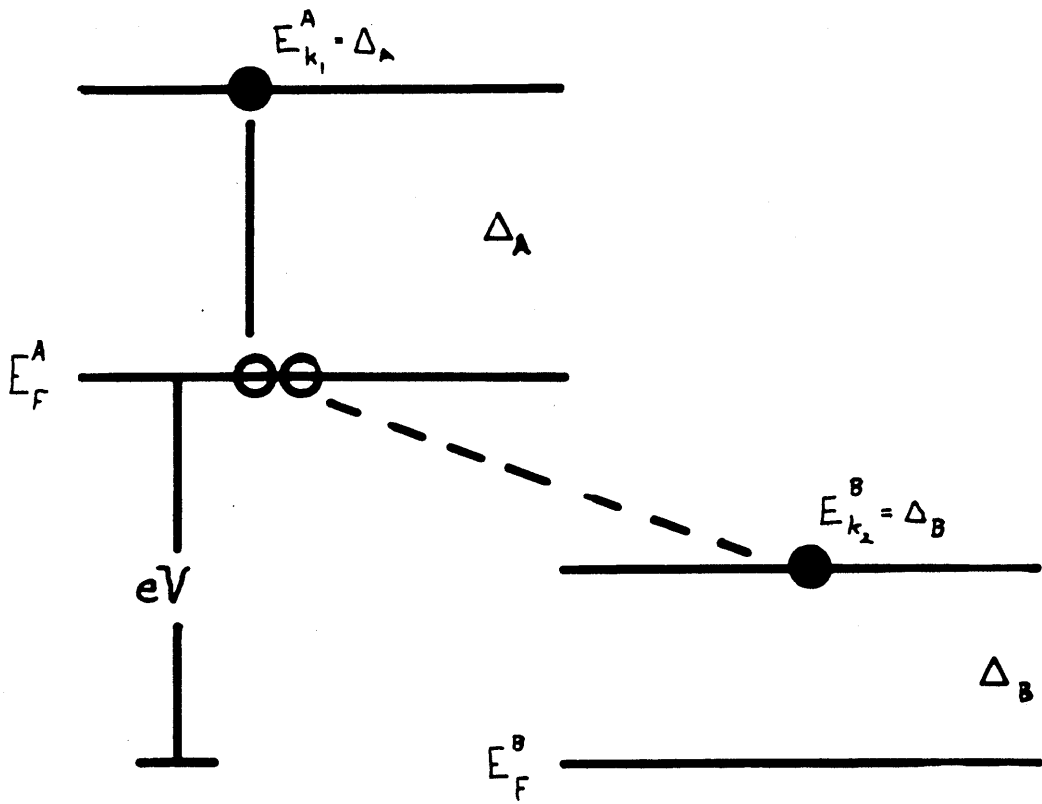


FIGURE 4: (a) The Occupation of Quasiparticle Levels at Finite Temperature.

(b) Tunneling at Finite Temperatures.

This is the origin of the "difference" peak.

$$eV = \Delta_A - \Delta_B$$

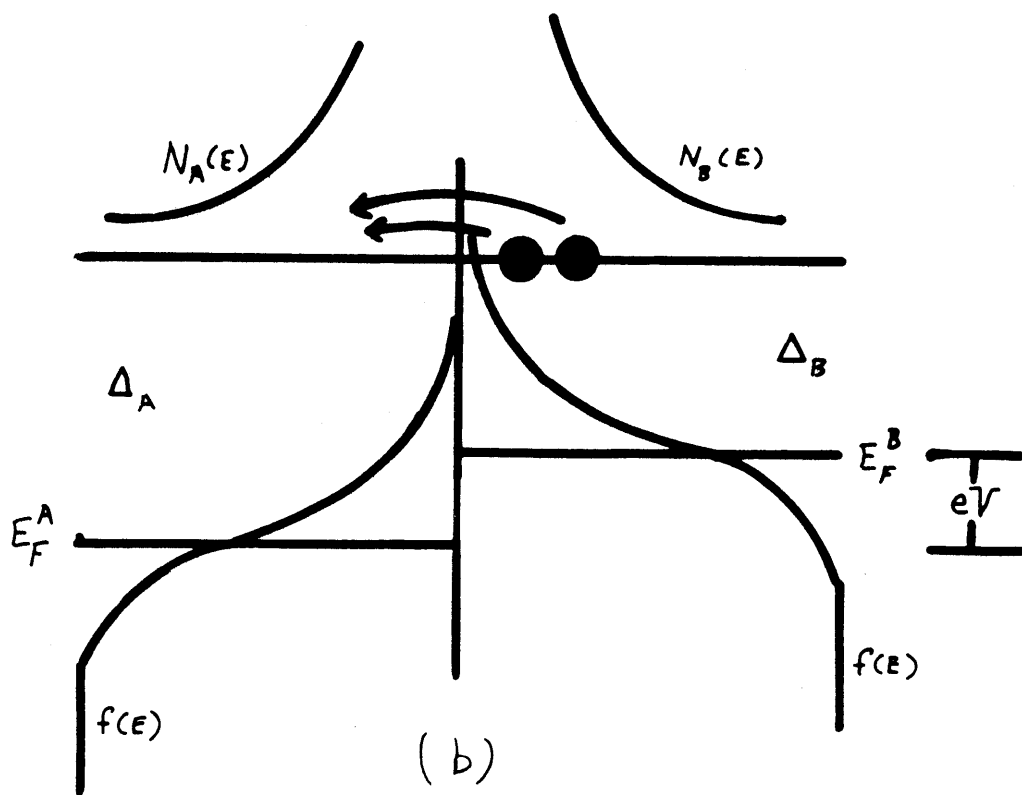
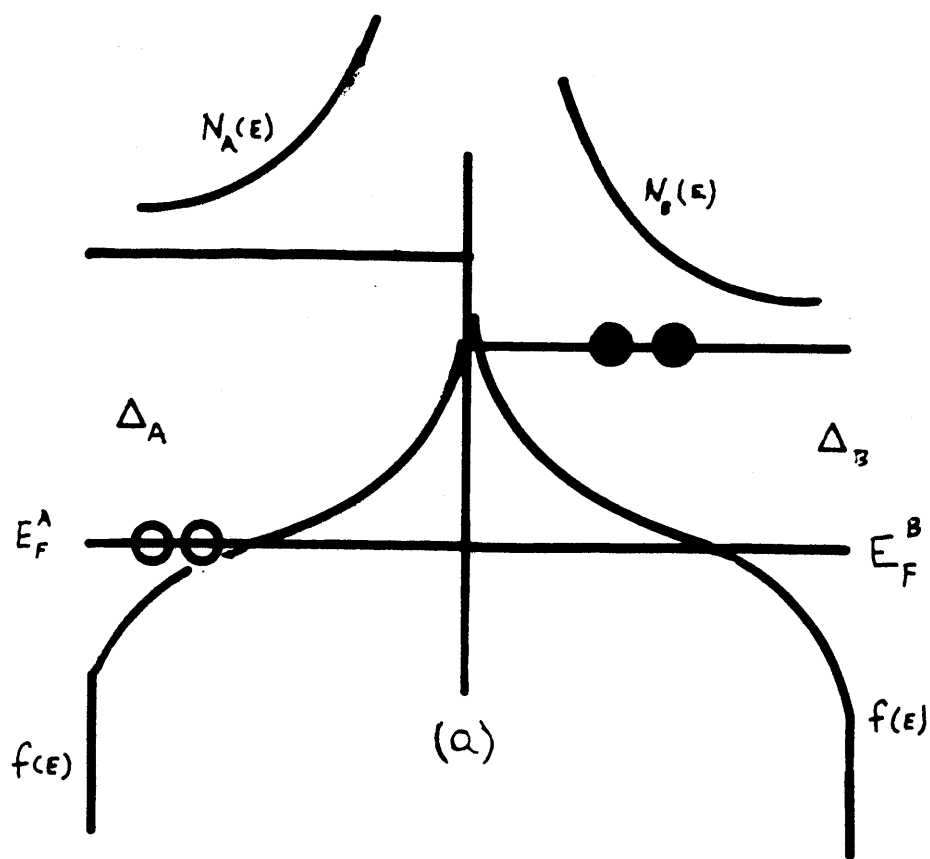
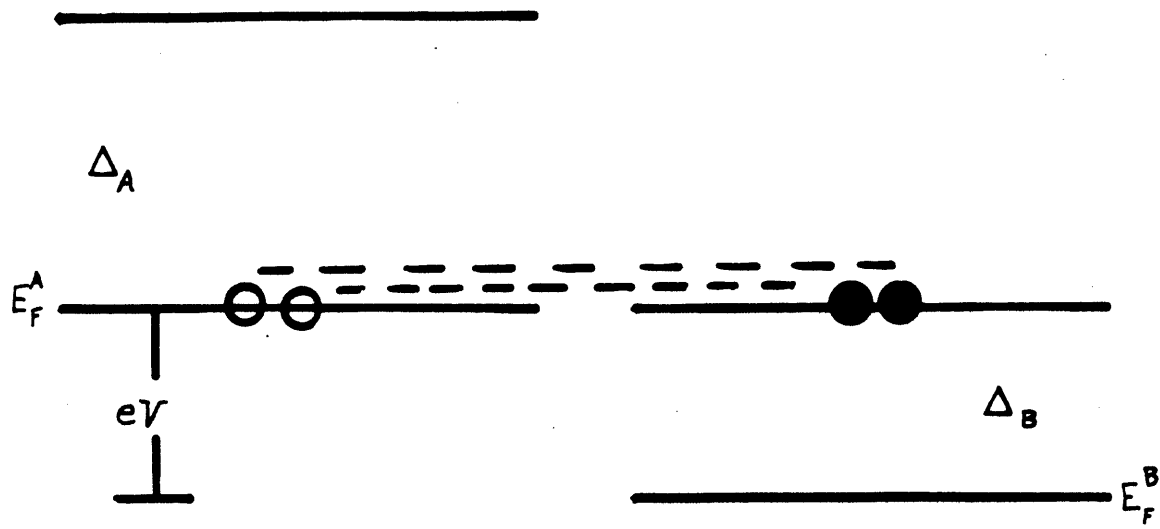


FIGURE 5: Multiparticle Tunneling

$$eV = \Delta_j.$$



OR:

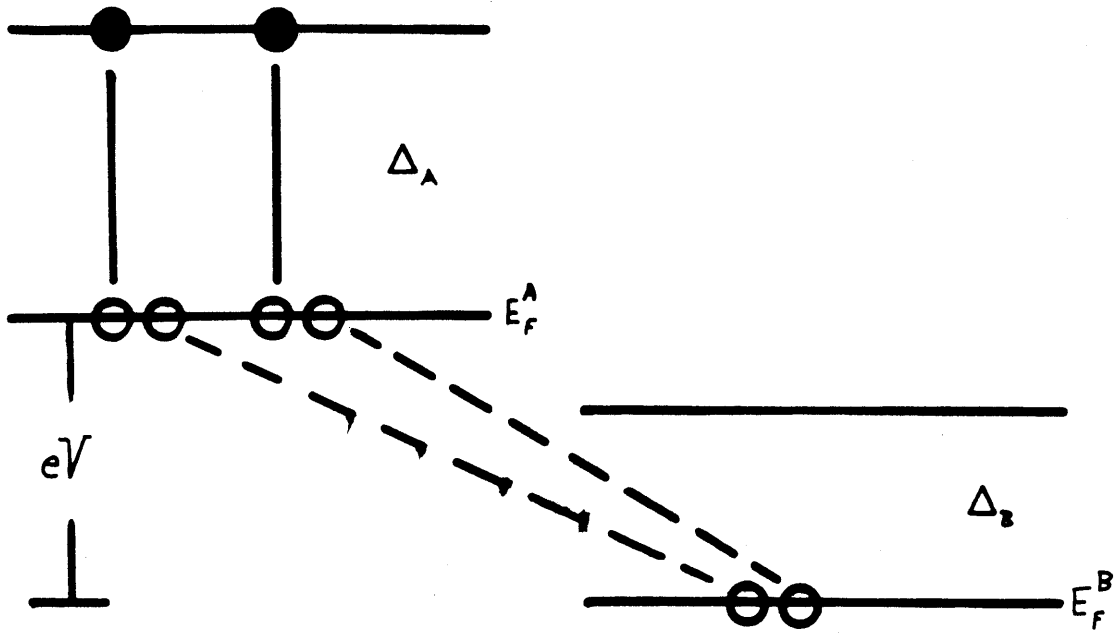


FIGURE 6: A Possible Quasiparticle Energy Diagram for a Two Band Superconductor.

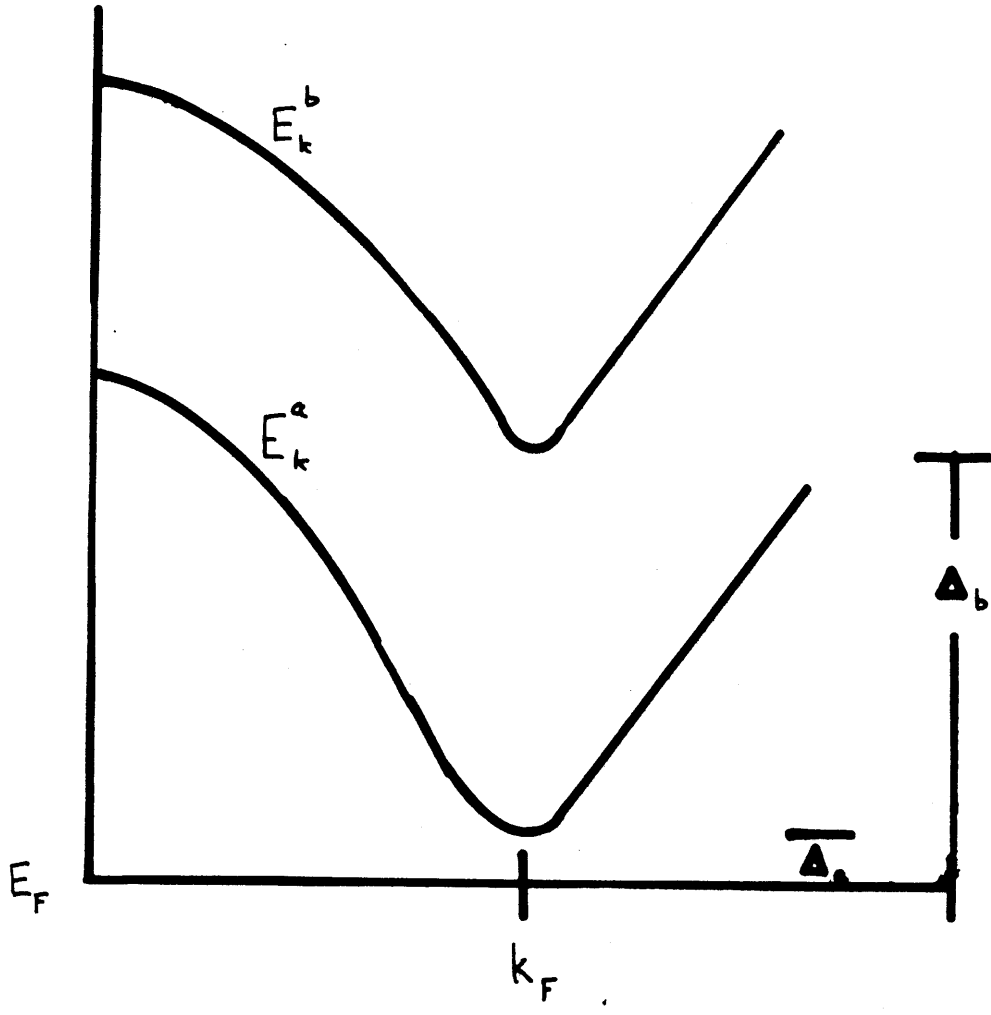


FIGURE 7: Tunneling in a Two Band Superconductor.

$$eV = \frac{\Delta_a + \Delta_b}{2}$$

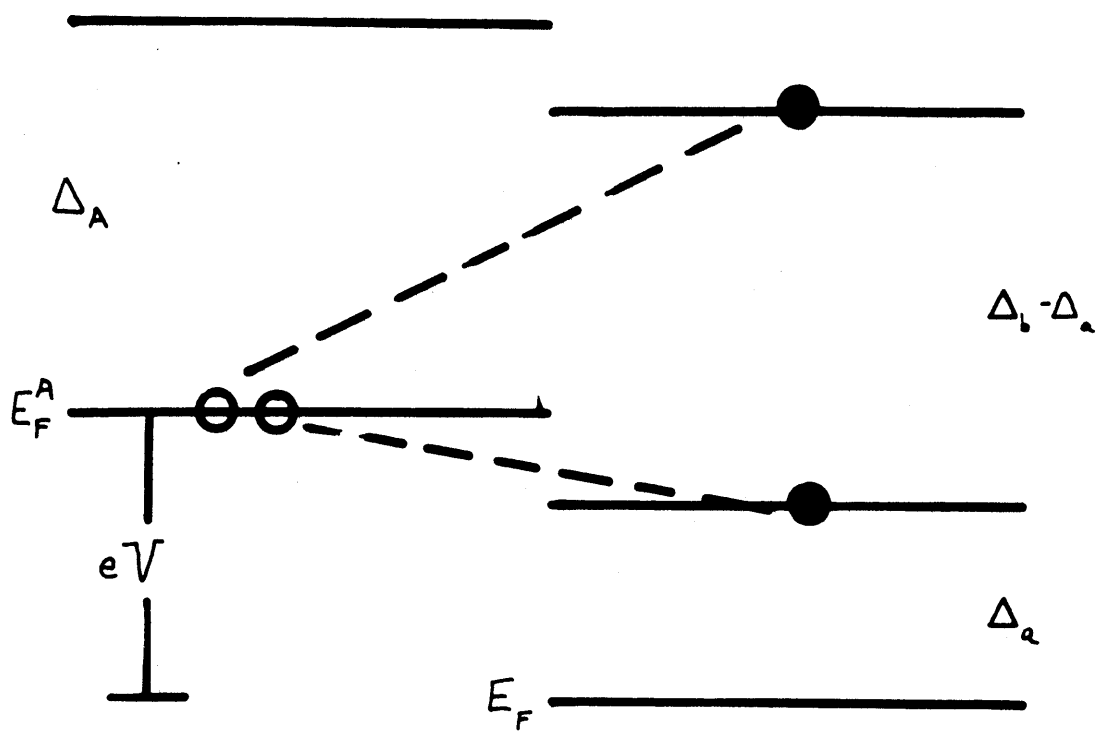


FIGURE 8: (a) Josephson Effect.

$$eV = 0$$

(b) Excitation of Quasiparticles by Absorption of Photons or Phonons.

$$eV = \frac{2\Delta_i}{2n}$$

(c) Photon or Phonon Assisted Tunneling.

$$eV = \frac{\Delta_1 + \Delta_2}{1 + 2n}$$

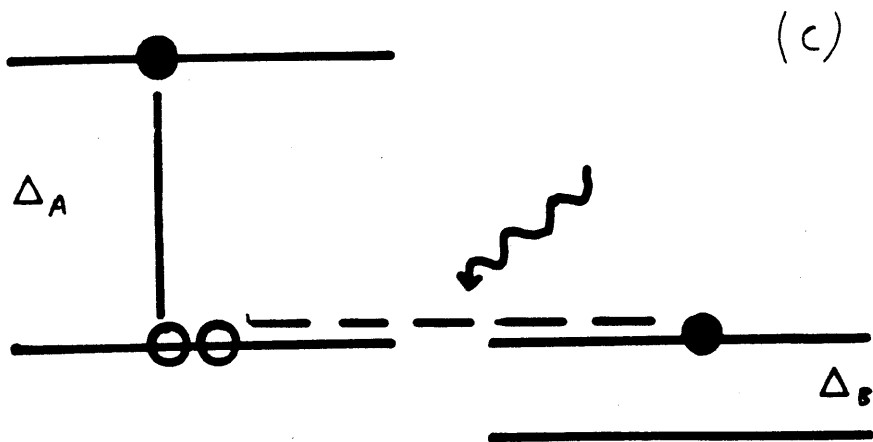
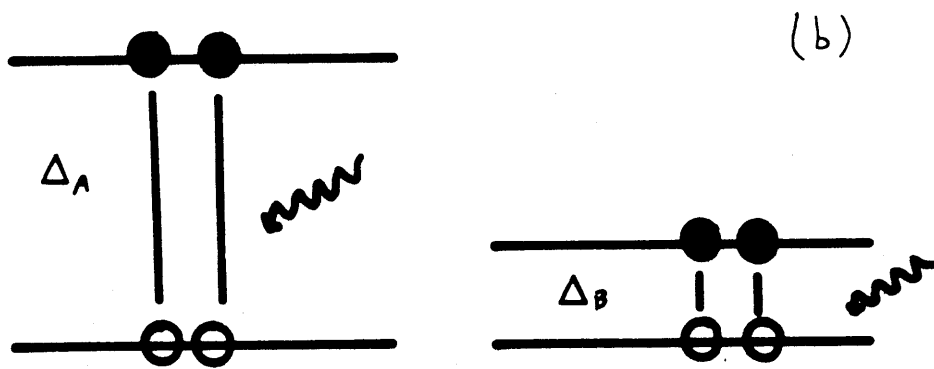
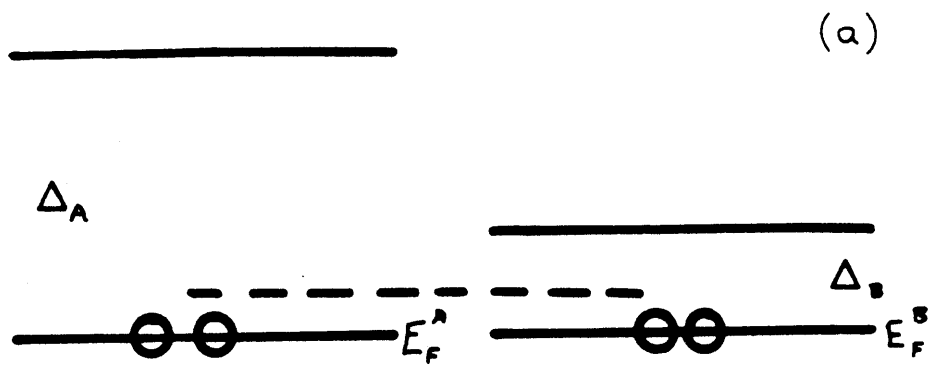


FIGURE 9: Test Sample Mounted for the Helium-3 Cryostat.

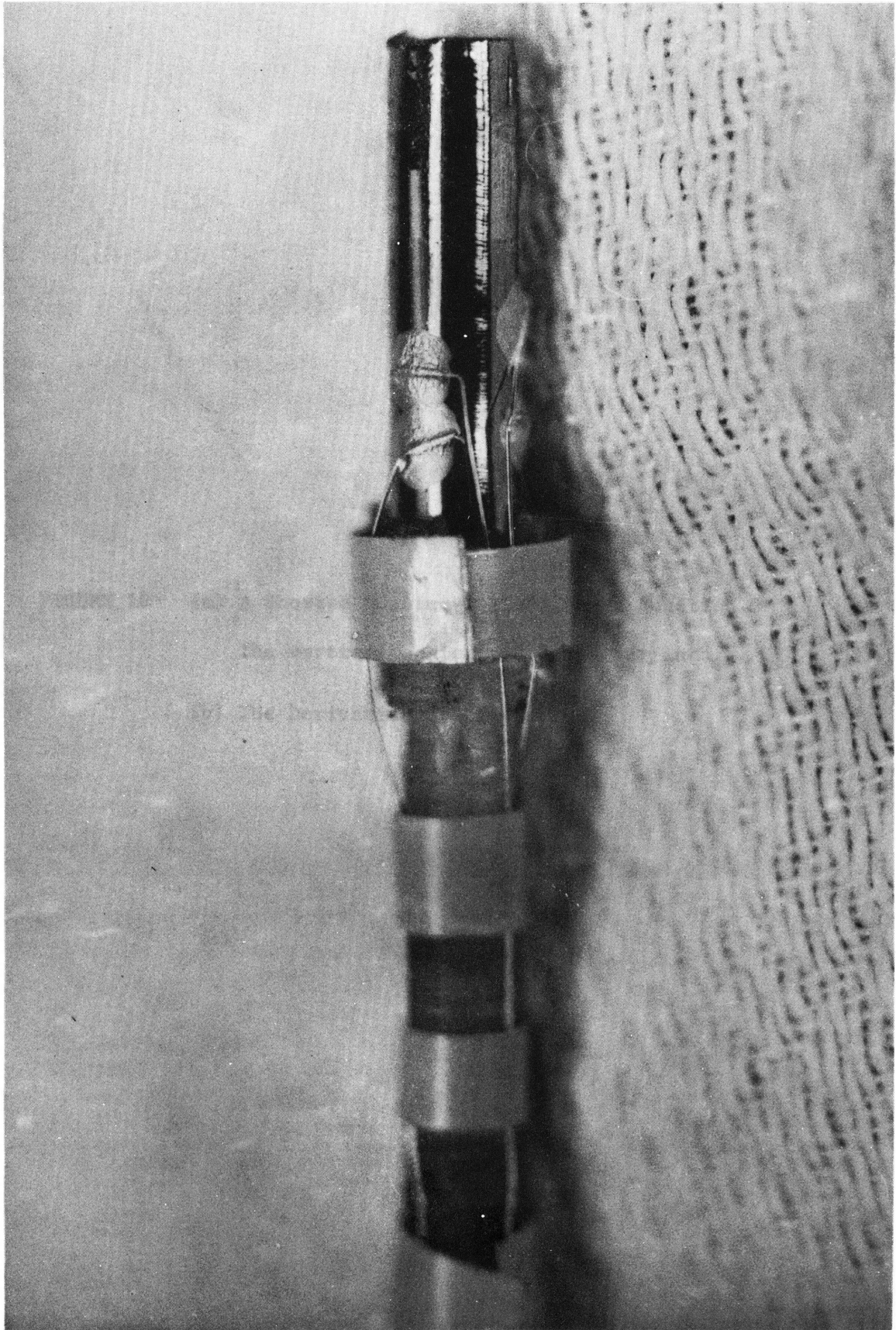
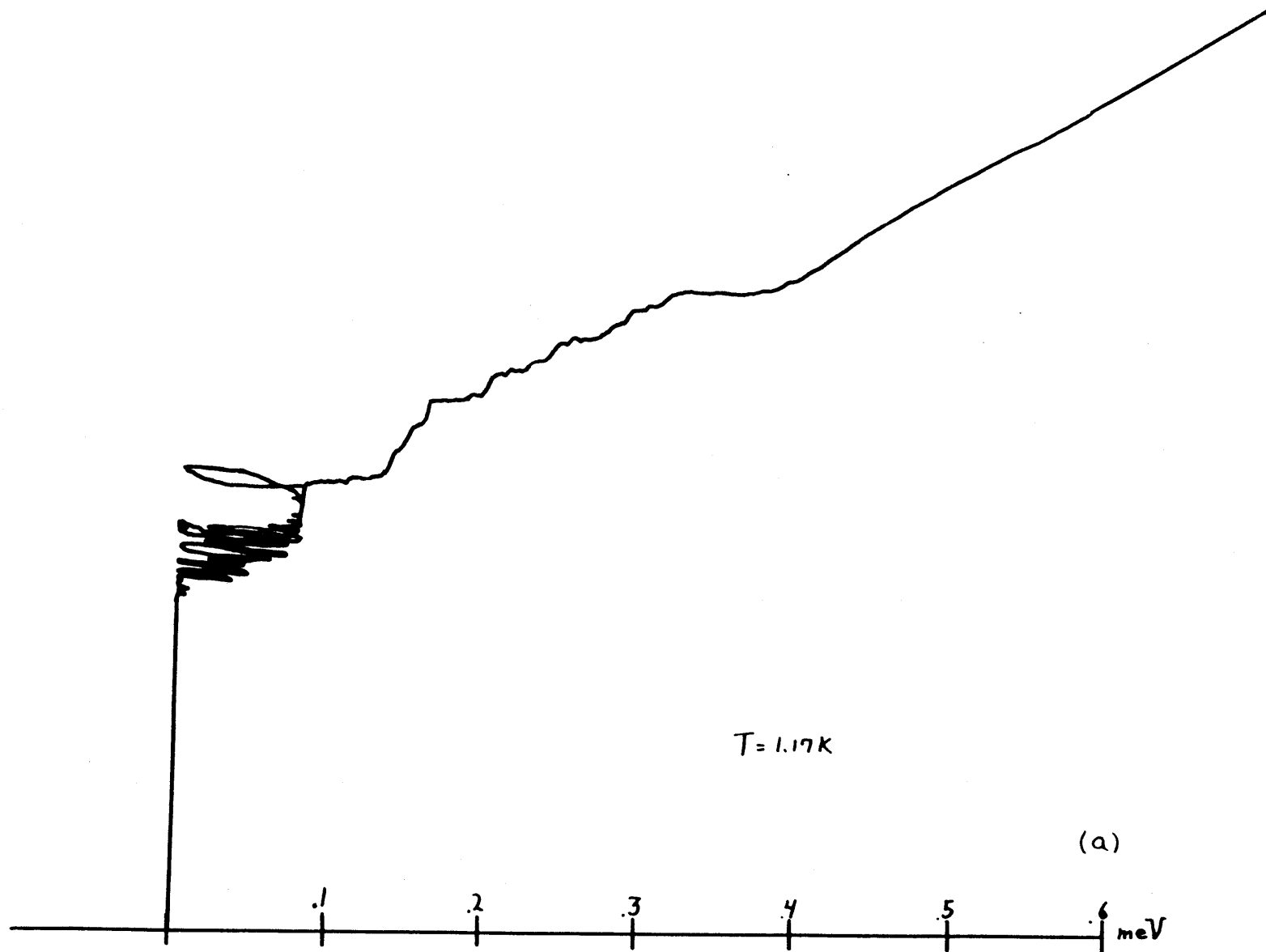


FIGURE 10: (a) A Shorted Niobium-Indium Tunnel Junction.

The vertical scale is 0.5 meV per inch.

(b) The Derivative of Figure 10a.



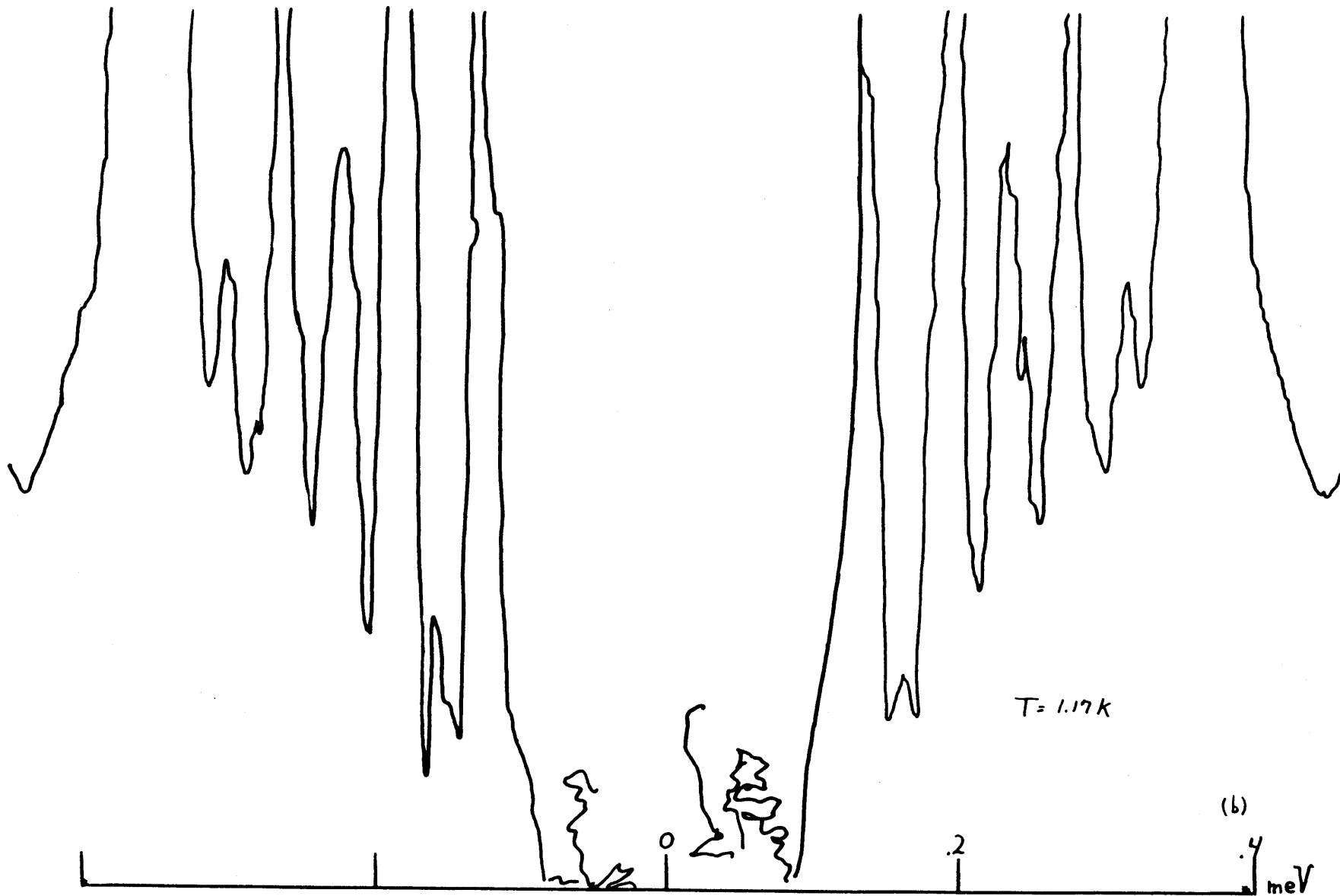
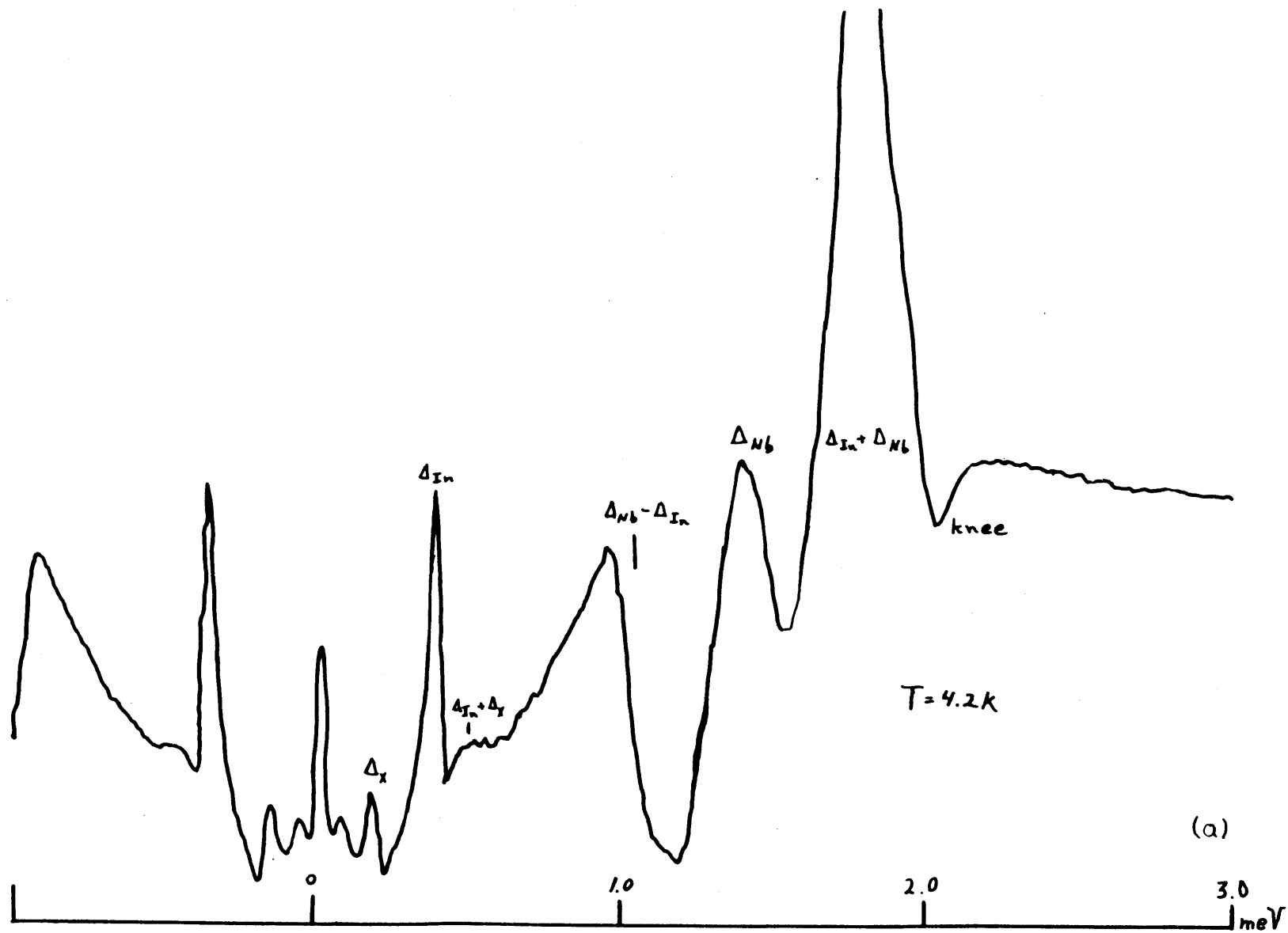


FIGURE 11: (a) The Same Junction as in Figure 10 but with a Better Oxide.

This is the derivative at 4.2K.

(b) As in (a), but at 1.17K

The vertical scale of the I-V curve is 0.1 meV. The difference peak has vanished.



(a)

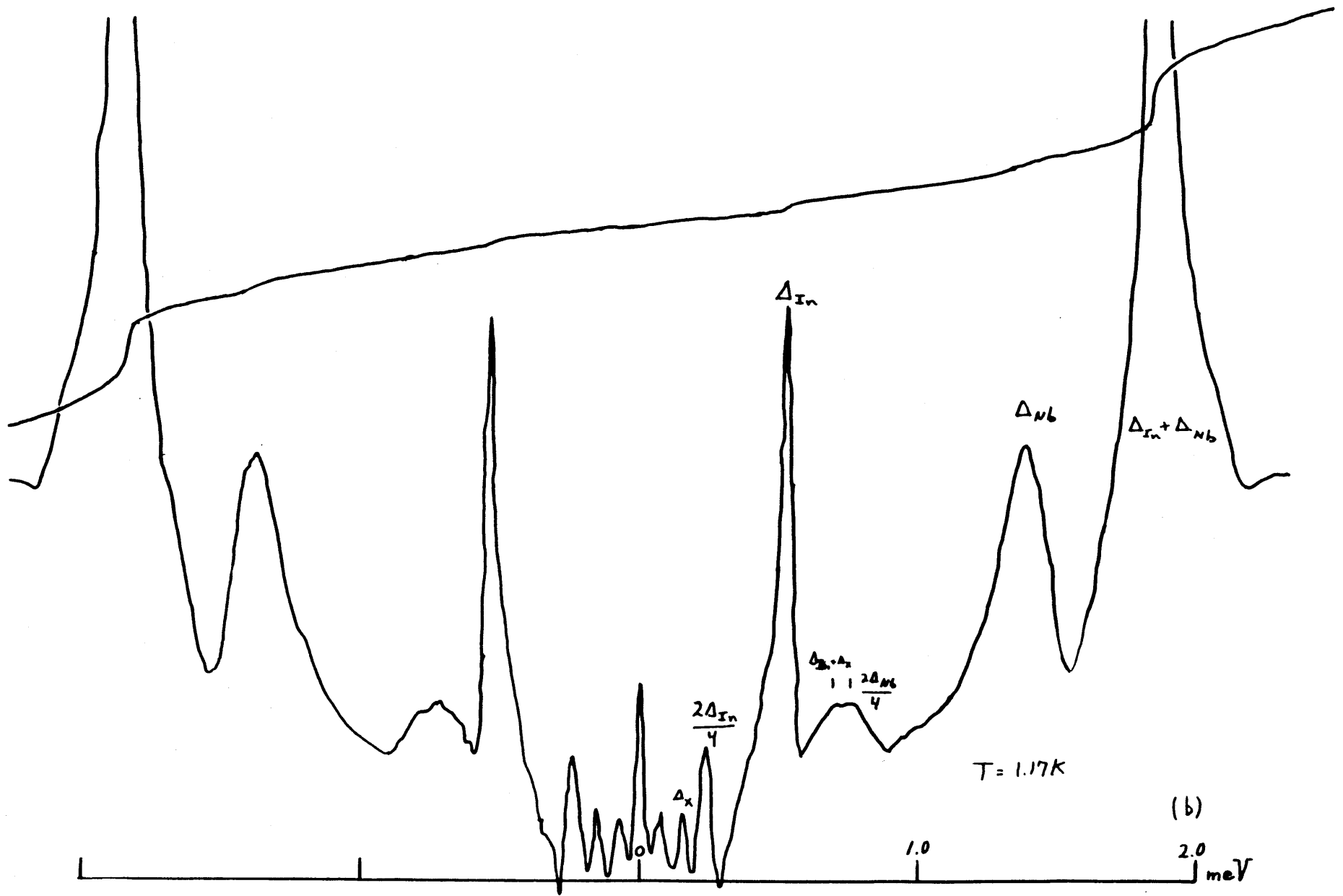


FIGURE 12: Structure in a Niobium-Indium Tunnel Junction
at 0.48K .

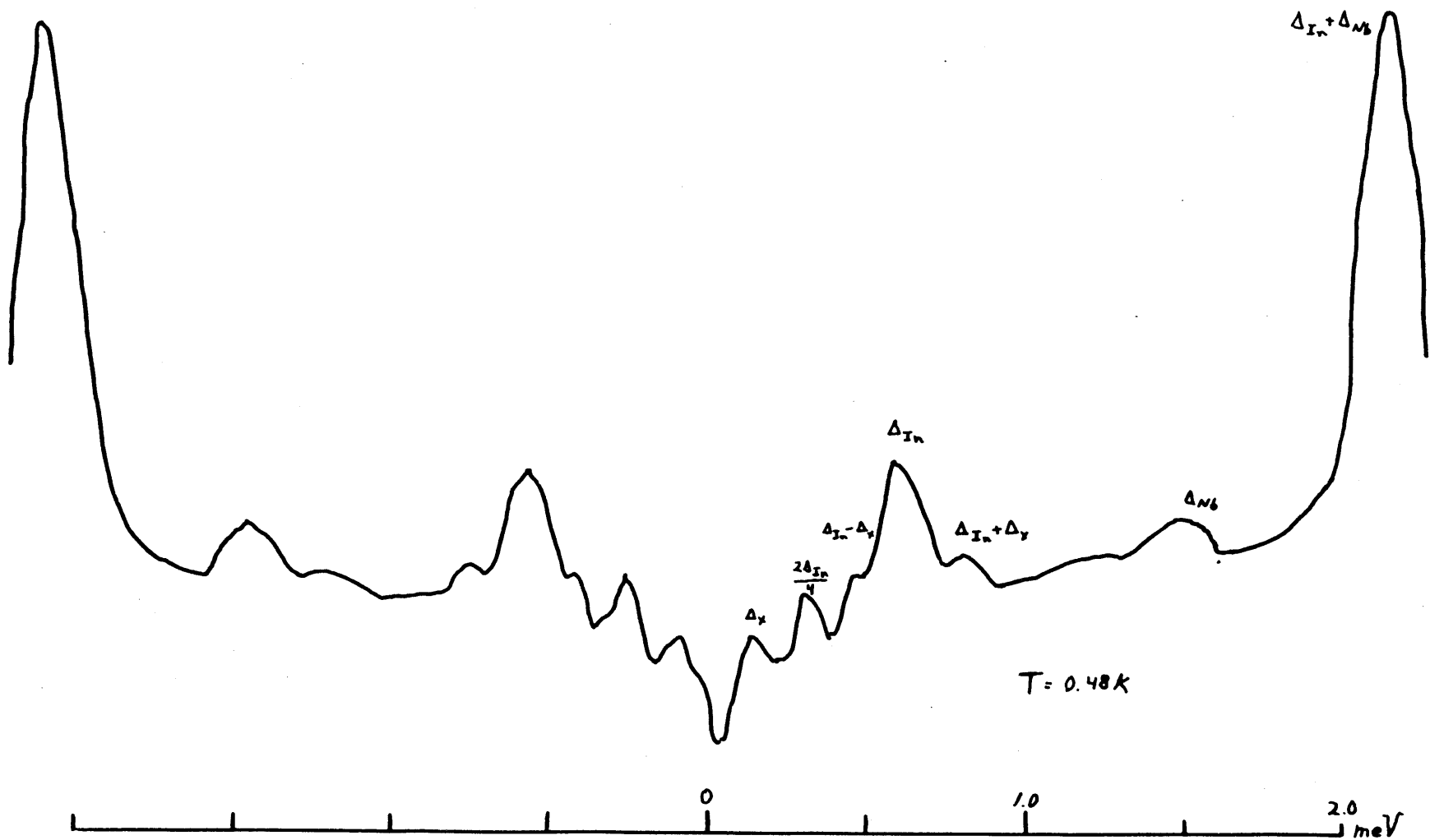


FIGURE 13: Type I Lead Junction.

The top I-V curves have a vertical scale of 0.1 meV per inch.
The lower curves have a vertical scale of 0.5 meV per inch.

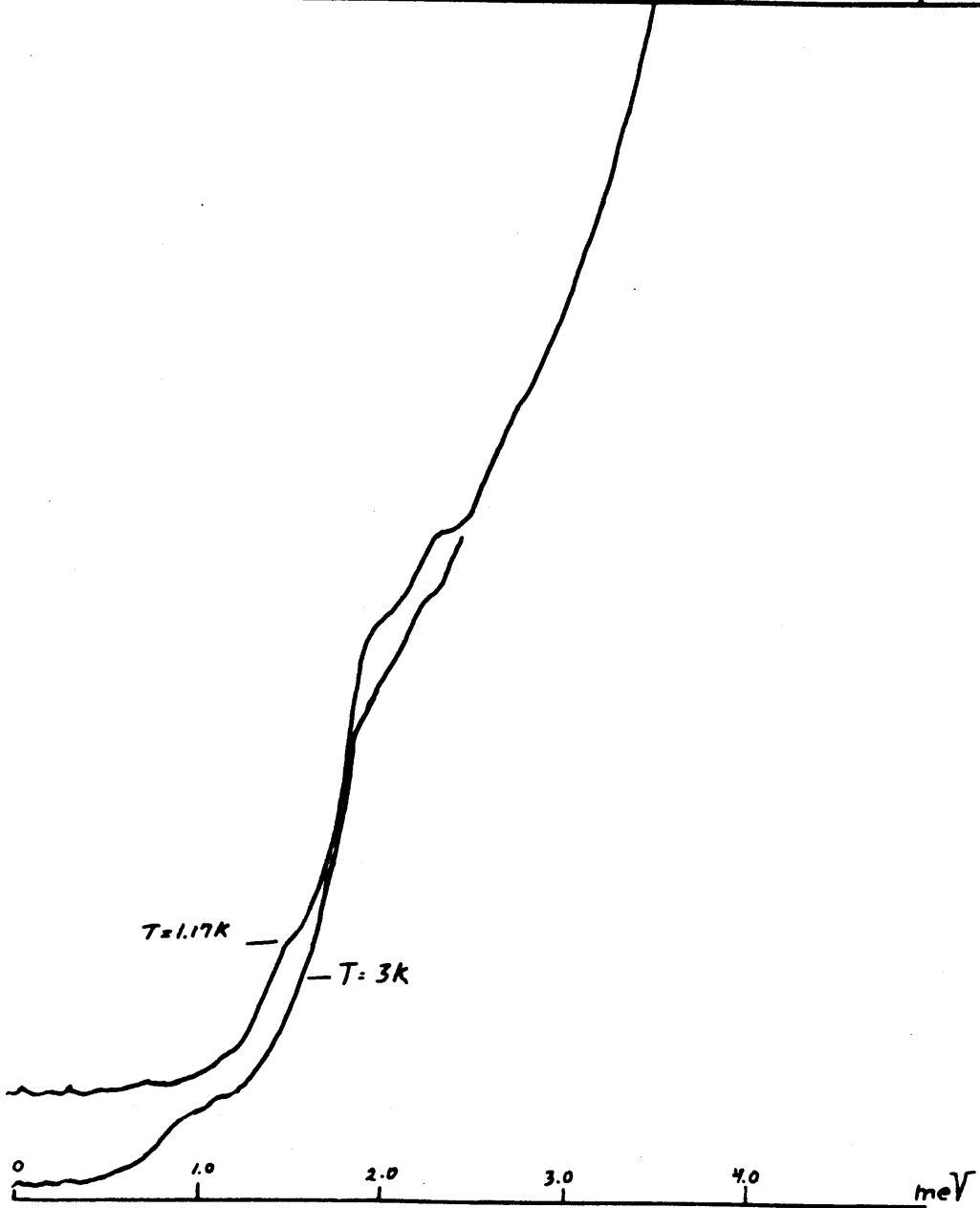
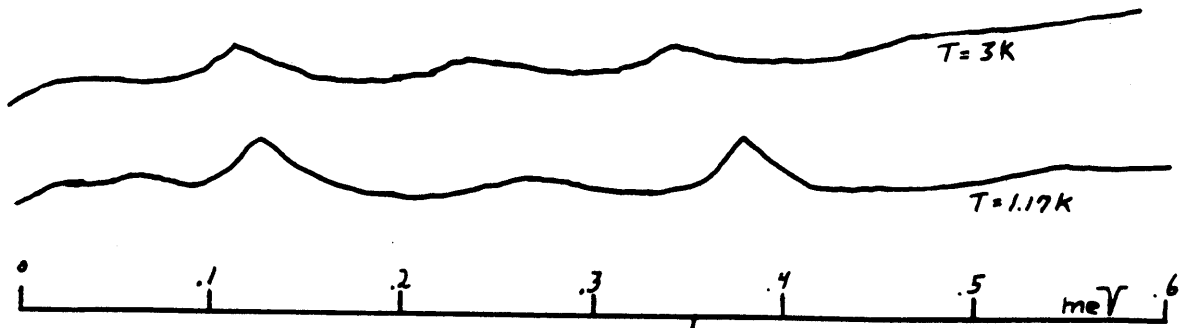
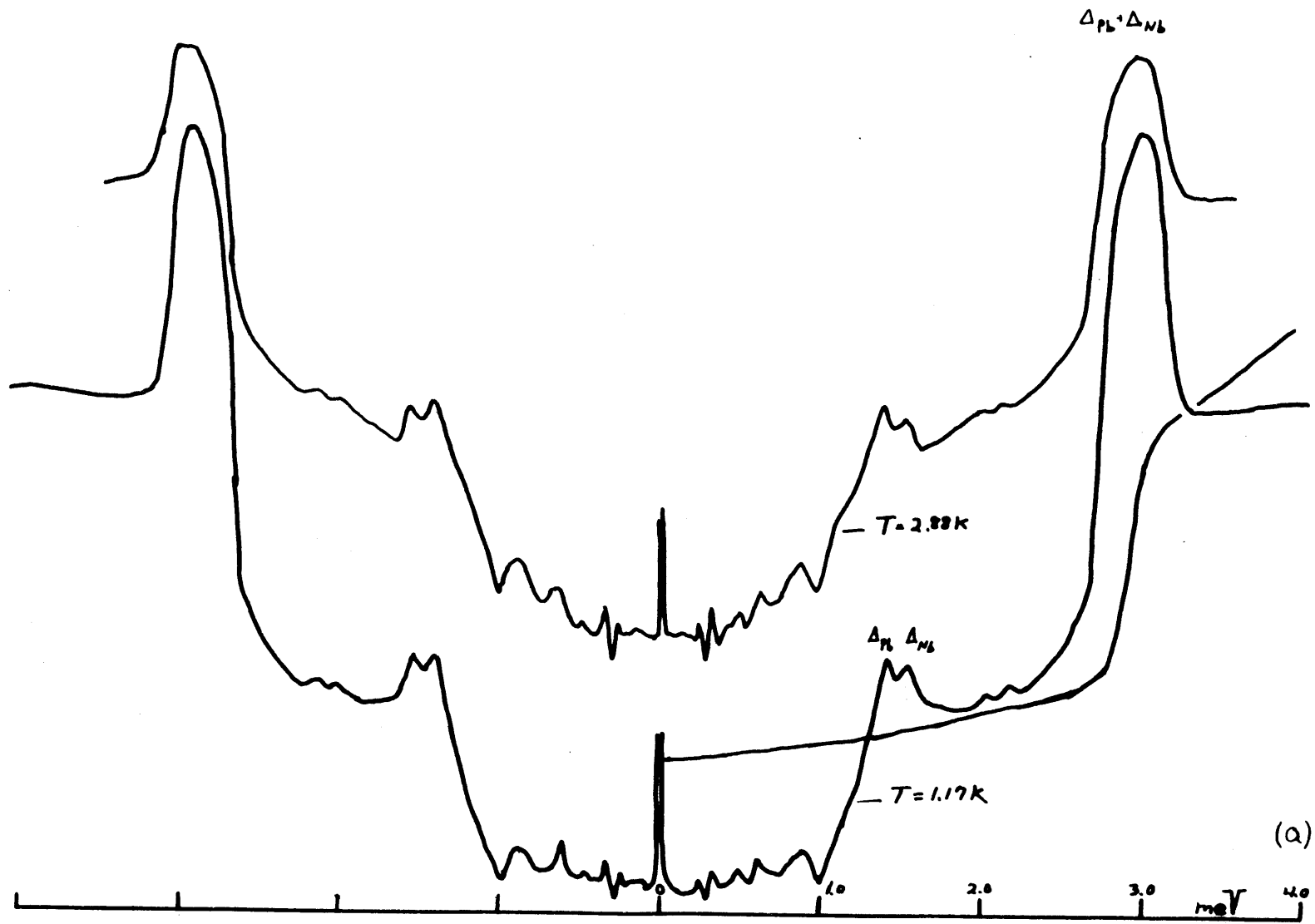


FIGURE 14: Type II Lead Junction.

- (a) Derivative of a typical junction. The vertical scale of the I-V plot is 5 meV per inch.
- (b) Type II junction showing a broadened sum peak.



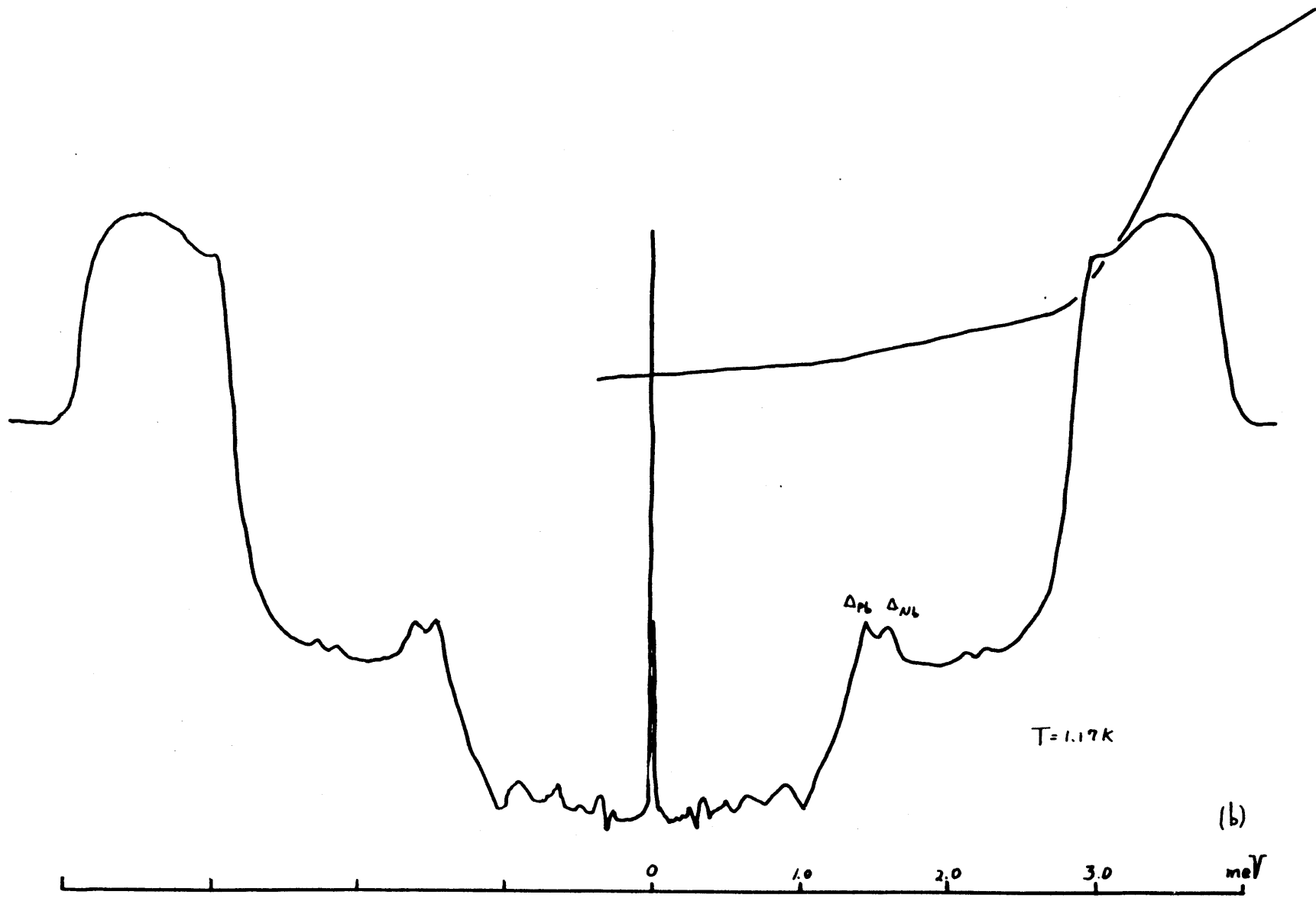
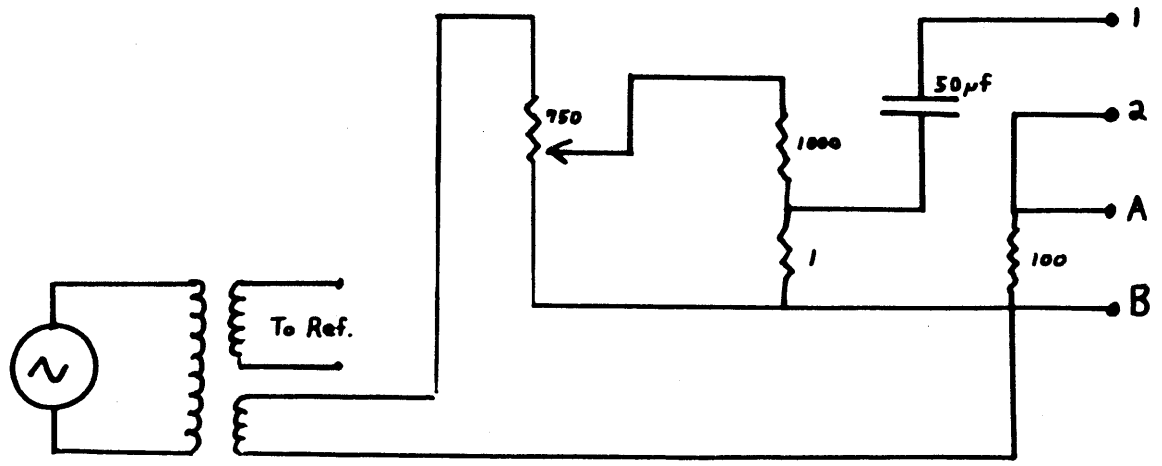
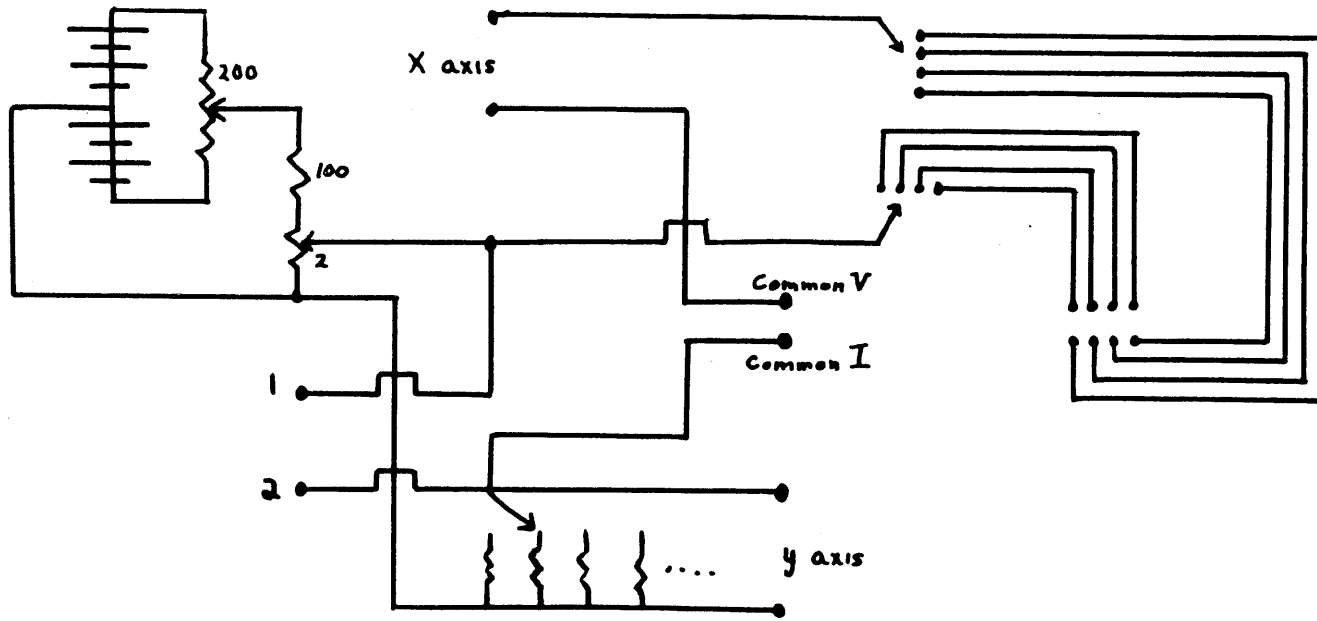
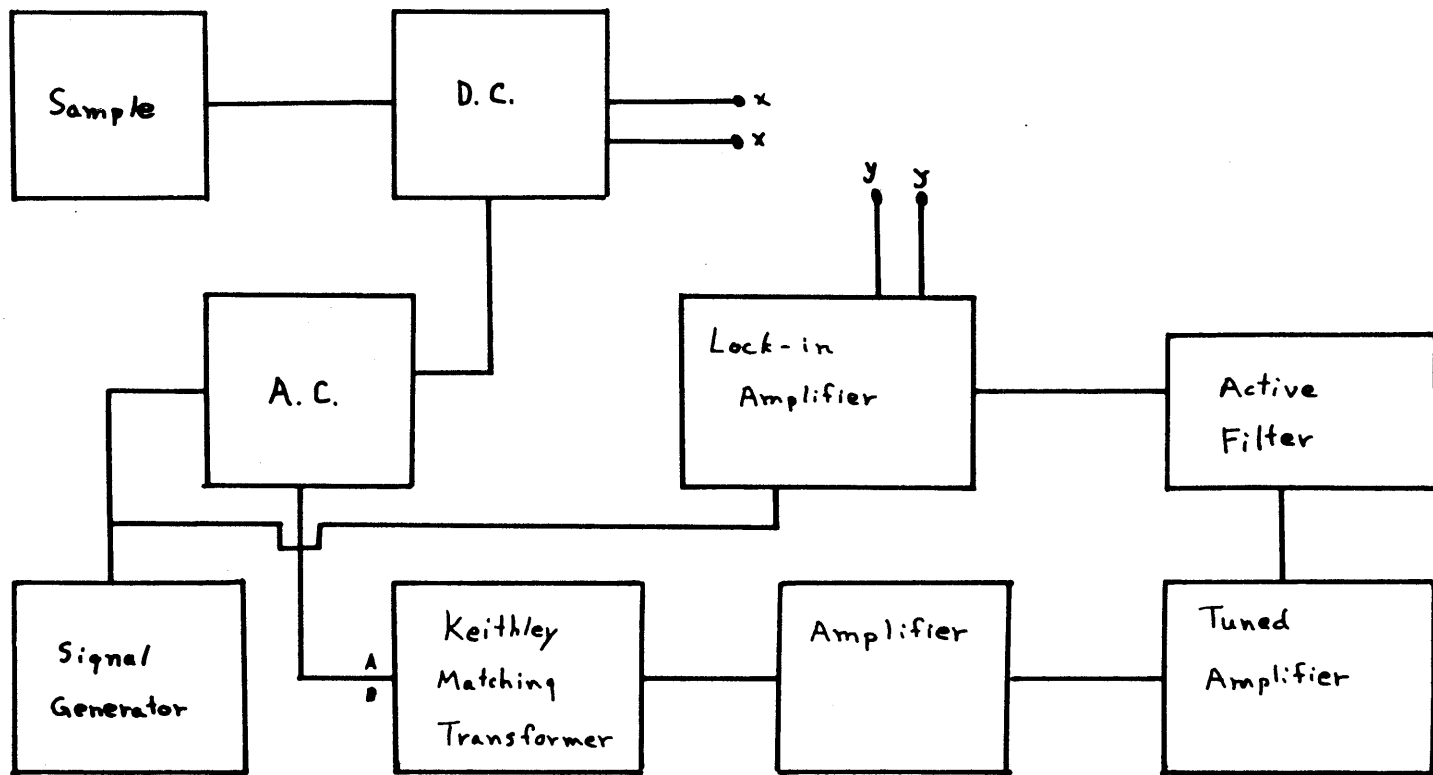


FIGURE 15: (a) Circuit Diagram of the Voltage Sources.

(b) Detection Network.



(a)



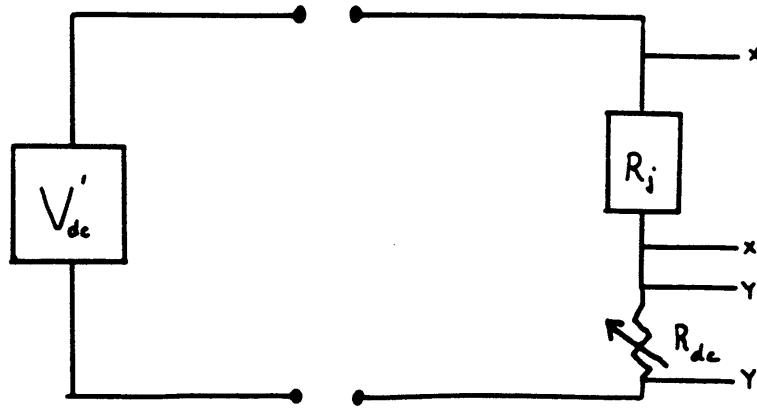
(b)

FIGURE 16: Equivalent Circuits.

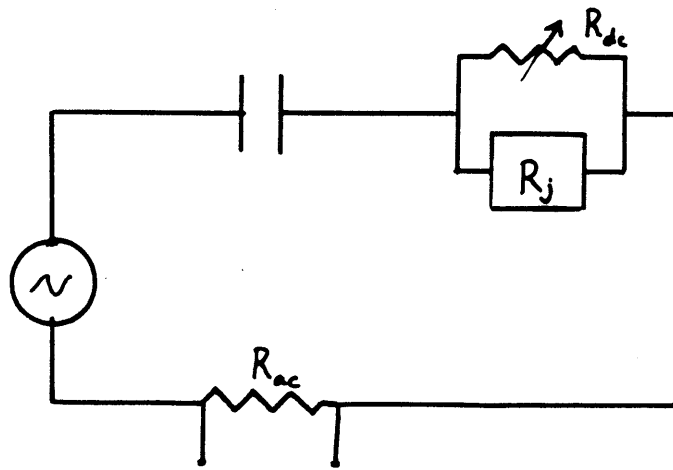
(a) D.C. Network.

(b) A.C. Network.

(a)



(b)



OR:

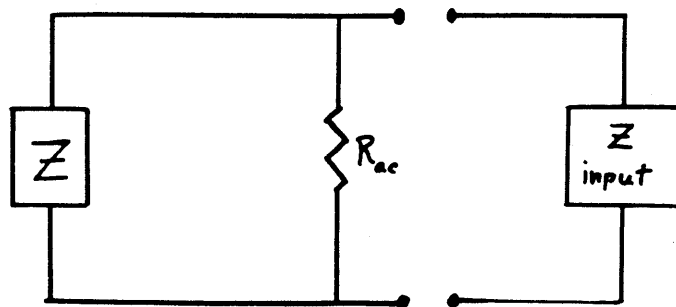
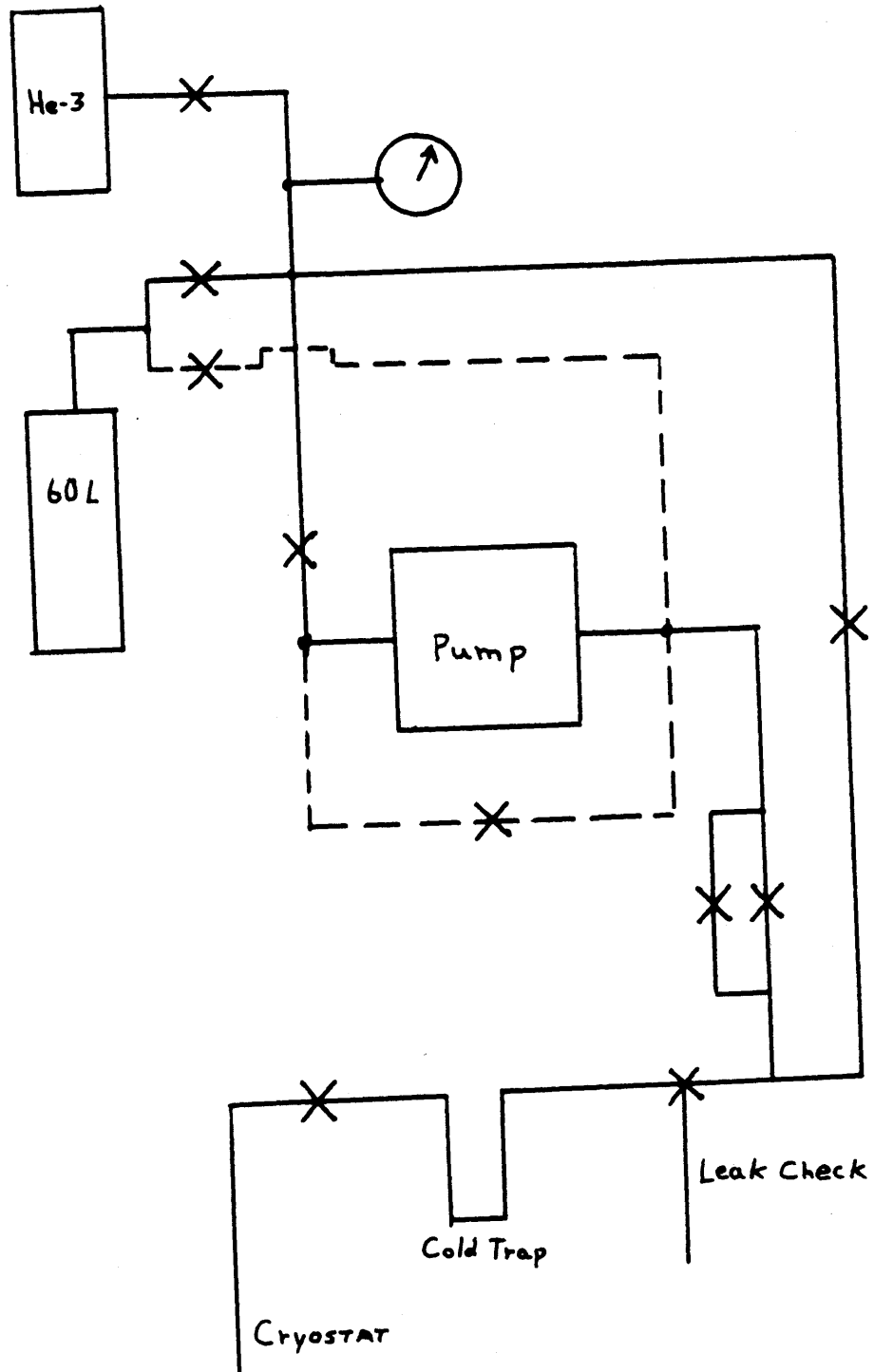


FIGURE 17: The Helium-3 Gas Handling System

The dashed lines are used only after the completion of a run.



APPENDIX

CRYOGENICS

The initial attempt to test niobium at low temperatures involved placing the sample inside the "pill" of an adiabatic demagnetization apparatus. Unfortunately there is a thermodynamic restriction; when the field is removed during the cooling cycle, the superconducting crystal heats up. Because the niobium crystal is relatively large and has very small thermal conductivity when superconducting, thermal drift of extremely long duration results.

Reaching low temperatures therefore required a helium-3 cryostat. As simplicity was desired, a "one-shot" device was constructed and is described below.

The cryostat proper is constructed of thin wall, 3/8" I.D., 304 stainless steel. The bottom six inches is enclosed by a 3/4" I.D. 304 stainless steel vacuum jacket. The enclosed section of the inner cryostat is short enough to allow condensation of the He-3 gas at 1 K, yet long enough to maintain thermal isolation sufficient to maintain temperatures of less than 0.5 K for several hours.

The sample is mounted inside the cryostat on a nylon post at the end of an 1/8" I.D. 304 stainless steel tube. The nylon post maintains thermal isolation of the sample and extends above the vacuum jacket. The lower end of the post is detachable by means of a niobium screw to facilitate sample mounting and provide additional thermal isolation. Six leads from the sample are brought out inside the small tube. Before entering the tube, they are thermally anchored to the He-4 bath at 1 K by a copper spring.

Several radiation shields are attached farther up the sample holder, optically isolating the lower cryostat. They are located above the He-4 bath to prevent He-3 condensation at this point. The wires are brought out through a vacuum-sealed header attached to the sample tube.

The temperature may be measured either by a thermocouple gauge on the header, or by a calibrated carbon resistor mounted on a copper block at the bottom of the inner cryostat tube. The cryostat tube is of sufficient diameter that the temperature as measured by the resistor agrees with the pressure (temperature) measured at the top of the inner tube 42 inches away. That is, the gas flow is in the viscous region.

Operation:

To prepare for a run, the inner cryostat and vacuum jacket are pumped hard by a diffusion pump and checked for leaks. Liquid helium is admitted to the dewar and allowed to cover the lower part of the cryostat. A final leak check is performed and the vacuum jacket and cryostat sealed. He-3 gas is bled into the inner cryostat. The gas boils off most of the initial charge of liquid helium. After a cooling period, the He-4 level is raised to the top of the dewar and then pumped on to attain 1 K. As the inner cryostat cools, the He-3 condenses. After about 30 minutes, the He-3 is pumped on from the pumping station. Temperatures of 0.48 K are maintained for several hours under nominal power loads of several microwatts at the sample junction.

Pumping Station:

The gas handling system is built around a 5 cfm sealed rotary pump. The entire system is carefully sealed to prevent loss of the expensive isotope. (\$110 per liter STP). A block diagram is shown in figure 17. The cold trap is essential to remove any extraneous vapors, such as oxygen and oil, which may limit the ultimate temperature attainable. A cold trap is also placed on the exhaust (tank) end of the pump to prevent contamination by oil. A by-pass valve on the pump is opened at the end of a run to equalize pressures on either side of the pump. The large (60 liter) storage tank is opened after the small He-3 reservoir is filled and sealed. The volume is larger than that of the system and, hence, may be used to purge the lines of He-3. It must be pumped out before each run.

ELECTRONICS

A complete circuit diagram is shown in figure 15. The d.c. network provided a low impedance voltage source and a bias voltage during derivative measurements. The a.c. circuit acted as a voltage source and detector of a small a.c. signal at a 100 ohm resistance. The detection circuitry amplified and refined this signal.

D.C. Network

The d.c. controller allowed the selection of one of four junctions and a variety of series impedances acting as current sensors. The battery arrangement allowed passing the I-V curve continuously through the origin to more accurately determine the zero point. A sensitivity of 10 micro-volts for the d.c. bias is potentially available but, in practice, thermal noise reduces the sensitivity to around 40 micro-volts.

The junction resistance is obtained by measuring the reciprocal slope of the I-V plot above the sum peak and multiplying by the series impedance used. A series impedance equal to that of the junction resolves the most detail.

An equivalent circuit for the d.c. network is shown in figure 16a. R_j is the junction impedance which is constant (ignoring phonons) above the sum peak and R_{dc} is the series impedance (current sensor). We have then:

$$V'_{dc} = I(R_j + R_{dc})$$

The voltages developed are:

$$\text{and } V_x = I R_j$$

$$V_y = I R_{dc}$$

where x and y refer to recorder terminals. Solving for the current:

$$I = V_x / R_j$$

hence; solving for R_j :

$$R_j = \left(\frac{V_x}{V_y} \right) \cdot R_{dc}$$

A.C. Network:

The a.c. circuit supplies a small (10 micro-volt) a.c. voltage to the junction. The output of the signal generator is stepped down by the appropriate winding on a matching transformer and further attenuated by a voltage divider network. The 50 f capacitor acts as a d.c. block while offering little impedance or phase shift to a 5 kHz signal.

The a.c. current returning from the junction sees the 100 ohm resistive output impedance R_{ac} in parallel with what is effectively the d.c. resistance bank (the impedance of the coupling capacitor and the a.c. signal source are very small) and the reactive input impedance of the Keithley matching transformer. The output impedance is chosen to match the Keithley transformer impedance and to be small compared to the junction impedance.

The equivalent circuit for the derivative network is shown in figure 16b. We demonstrate first that R_{ac} must be small compared to R_j . R_j drops at the tunneling point, i.e. , the conductance increases. (note that we are seeking the differential conductance) We first set R_{dc} equal to R_j and call the new "junction impedance" R_j' . Referring to figure 16b, we find:

$$V_{\text{input}} = I (R_j' + R_{ac})$$

$$V_{\text{output}} = I R_{ac}$$

and

$$\Delta I = -V_{in} / (R_j' + R_{ac})^2 \cdot \Delta R_j'$$

or:

$$\Delta V_{out} = \Delta I \cdot R_{ac} = -V_{in} / (R_j' + R_{ac})^2 \cdot \Delta R_j' \cdot R_{ac}$$

Hence:

$$\Delta I / \Delta R_j' = -V_{in} / (R_j' + R_{ac})^2$$

R_{ac} should be small compared to R_j' which varies from point to point subject to the limitation of the input impedance of the matching transformer (33 ohms). It is obvious that a large change in current appears at the output if the break in the I-V curve is sharp (that is; R_j becomes very small at this point).

To this point, we have really treated only the magnitude of the signal to be detected without considering the phase of the signal at the detector. One must consider that the phase of an a.c. signal is given by:

$$\phi = \text{Tan}^{-1} (-1 / R_j' C \omega)$$

A sharp change in the junction impedance will shift the phase of the output signal. The lock-in amplifier is set so the frequency and phase of the signal from the junction matches that of the reference signal at $eV=0$. Any phase change caused by a conductance change at the junction will appear as a drop in the output of the lock-in amplifier.

The Derivative:

We digress to discuss the need for a small a.c. signal to point

out how a derivative is generated. We note that a small perturbation about some arbitrary point may be expanded in a Taylor series about that point:

$$f(a+h) = f(a) + hf'(a) + \frac{h^2}{2!} f''(a) + \dots$$

We express the current (point by point) as a function of voltage with a small a.c. signal superimposed:

$$I = f(v) = f(v_0 + a \sin \omega t)$$

expanding;

$$I = f(v_0) + \left. \frac{df}{dv} \right|_{v=v_0} a \sin \omega t + \frac{1}{2} \left. \frac{d^2f}{dv^2} \right|_{v=v_0} a^2 \sin^2 \omega t$$

or simply:

$$I = I_0 + \frac{dI}{dV} + \frac{d^2I}{dV^2} + \dots$$

One detects the first derivative by setting the lock-in amplifier to the fundamental frequency and the second derivative by setting it at the first harmonic (2ω). Notice that for the expansion to succeed, or equivalently, to detect very small changes in the I-V curve, the a.c. signal level (measured by a) must be much smaller than the change in voltage over the range of interest.

BIOGRAPHICAL

The author was born in May, 1943, attended public schools and graduated from Fullerton Union High School, California, in 1961. He attended the Massachusetts Institute of Technology receiving an S.B. in Physics in 1965.

The author was employed as a teaching assistant during his four years of graduate study and won the Goodwin Medal. He is a member of the American Physical Society and Sigma Xi.